MSA patients, 62.3 ± 7.4 years; PD controls, 68.5 ± 8.3 years vs. PD patients, 68.6 ± 7.9 years; CHF controls, 59.1 ± 16.0 years vs. CHF patients, 66.1 ± 14.8 years). The age distributions for the control groups were not significantly different from those for the patients' groups. Mean duration since MSA diagnosis was 3.3 ± 2.1 years (range, 1–9 years; **Table 1**). Mean duration since PD diagnosis was 10.7 ± 9.1 years (range, 2–31 years), and the mean Hoehn and Yahr score was 3.6 ± 0.7 (range, 3–5; **Table 2**).

CONVENTIONAL HRV INDICES

Table 3 presents HRV indices derived from HRV recordings from MSA patients and age-matched healthy control subjects, together with the bootstrap estimators for the healthy controls. Compared with the control group, the MSA patients showed significantly decreased HRV as indicated by lower SDNN, SDANN, and RMSSD values, reduced power in all spectral bands (HF, LF, VLF, ULF), and lower DC and AC. Indices such as LF/HF and DFA α_1 were also significantly decreased. Compared with the control group, the PD patients showed significant decreases only in LF and VLF power and significantly lower DC and AC (**Table 4**). LF/HF and DFA α_1 were significantly decreased. As shown in **Tables 3** and **4**, these findings were largely supported also by comparing mean values for the patient groups with 95%-confidence intervals of the bootstrap estimators. **Table 5** presents the HRV indices in CHF patients and age-matched healthy control subjects. Compared with the control group, both surviving and non-surviving CHF patients exhibited significantly decreased HRV as indicated by lower SDNN and SDANN, reduced power in LF, VLF, and ULF ranges, and lower

Table 3 | Heart rate variability measures in patients with multiple system atrophy (MSA) and age-matched controls.

	MSA ($n = 12$)	Age-matched control ($n = 69$)	*P* value	Bootstrap samples of age-matched control ($n = 12$)
Mean NN, ms	766 ± 89	775 ± 110	0.745	776 (723–832)
SDNN, ms	59.7 ± 23.0	90.4 ± 28.6	<0.001	89.0 (75.4–104.2)
SDANN, ms	19.9 ± 6.5	47.5 ± 28.7	<0.001	48.8 (35.5–64.5)
RMSSD, ms	13.6 ± 4.4	22.5 ± 11.4	<0.001	21.6 (16.3–27.6)
ln HF, ln ms^2	3.75 ± 0.90	4.97 ± 1.08	<0.001	4.93 (4.34–5.50)
ln LF, ln ms^2	4.02 ± 0.90	5.90 ± 0.97	<0.001	5.90 (5.39–6.36)
ln VLF, ln ms^2	5.92 ± 0.84	7.26 ± 0.81	<0.001	7.30 (6.89–7.72)
ln ULF, ln ms^2	7.78 ± 0.93	8.47 ± 0.64	0.029	8.45 (8.14–8.79)
LF/HF ratio	1.69 ± 1.24	3.28 ± 2.49	0.002	3.47 (2.25–4.87)
DC, ms	3.38 ± 0.98	6.23 ± 1.59	<0.001	5.82 (5.11–6.53)
AC, ms	−3.38 ± 0.93	−6.51 ± 1.77	<0.001	−6.13 (−6.94 to −5.28)
α_1	0.86 ± 0.24	1.17 ± 0.15	<0.001	1.21 (1.08–1.33)
α_2	1.23 ± 0.09	1.18 ± 0.04	0.118	1.19 (1.15–1.23)
λ_{25s}	0.46 ± 0.07	0.39 ± 0.07	0.005	0.38 (0.35–0.43)
λ^2-slope	−0.05 ± 0.12	−0.01 ± 0.08	0.309	0.00 (−0.04 to 0.04)

Fifth column shows mean value and 95%-confidence interval based on 2000 bootstrap samples. P< 0.05.

Table 4 | Heart rate variability measures in patients with Parkinson disease and age-matched controls.

	Parkinson disease ($n = 10$)	Age-matched control ($n = 60$)	*P* value	Bootstrap samples of age-matched control ($n = 10$)
Mean NN, ms	779 ± 118	780 ± 112	0.975	801 (717–885)
SDNN, ms	70.4 ± 33.5	91.6 ± 29.6	0.086	95.8 (76.1–118.7)
SDANN, ms	34.0 ± 26.7	46.6 ± 27.4	0.191	44.4 (30.3–62.2)
RMSSD, ms	18.2 ± 11.6	23.1 ± 12.8	0.240	26.3 (17.9–35.5)
ln HF, ln ms^2	4.21 ± 1.19	4.96 ± 1.13	0.089	5.00 (4.30–5.71)
ln LF, ln ms^2	4.22 ± 1.31	5.70 ± 0.97	0.006	5.69 (5.21–6.17)
ln VLF, ln ms^2	5.82 ± 1.20	7.17 ± 0.82	0.006	7.13 (6.68–7.56)
ln ULF, ln ms^2	8.15 ± 0.77	8.55 ± 0.64	0.148	8.66 (8.25–9.08)
LF/HF ratio	1.30 ± 1.03	2.62 ± 1.69	0.003	2.48 (1.60–3.54)
DC, ms	3.93 ± 1.41	5.46 ± 1.60	0.008	5.27 (4.45–6.11)
AC, ms	−4.03 ± 1.57	−5.80 ± 1.81	0.007	−5.74 (−6.80 to −4.73)
α_1	0.83 ± 0.28	1.12 ± 0.24	0.011	1.07 (0.96–1.19)
α_2	1.17 ± 0.08	1.19 ± 0.07	0.456	1.18 (1.14–1.23)
λ_{25s}	0.42 ± 0.09	0.40 ± 0.08	0.574	0.41 (0.37–0.46)
λ^2-slope	−0.01 ± 0.11	−0.02 ± 0.09	0.81	−0.02 (−0.06 to 0.03)

Fifth column shows mean value and 95%-confidence interval based on 2000 bootstrap samples. P< 0.05.

Table 5 | Heart rate variability indices in patients with congestive heart failure and age-matched controls.

	CHF (NS; $n=39$)	CHF (SV; $n=69$)	Control ($n=90$)	*P* value NS–SV	*P* value NS–C	*P* value SV-C
Mean NN, ms	758 ± 114	755 ± 140	782 ± 110	0.99	0.56	0.37
SDNN, ms	59.1 ± 31.1	59.7 ± 39.6	93.4 ± 29.0	0.99	<0.001	<0.001
SDANN, ms	33.0 ± 27.2	37.7 ± 33.6	51.6 ± 30.0	0.73	0.006	0.016
RMSSD, ms	37.6 ± 40.0	40.0 ± 48.3	24.5 ± 12.8	0.94	0.13	0.017
ln HF, ln ms^2	5.43 ± 1.57	5.30 ± 1.67	5.13 ± 1.12	0.89	0.82	0.75
ln LF, ln ms^2	4.97 ± 1.80	4.85 ± 1.63	5.97 ± 1.01	0.90	0.001	<0.001
ln VLF, ln ms^2	5.73 ± 1.36	6.04 ± 1.45	7.33 ± 0.83	0.40	<0.001	<0.001
ln ULF, ln ms^2	5.73 ± 1.23	6.04 ± 1.45	8.81 ± 0.64	0.66	<0.001	<0.001
LF/HF ratio	0.83 ± 0.79	0.93 ± 0.78	3.01 ± 2.31	0.95	<0.001	<0.001
DC, ms	3.39 ± 1.60	3.84 ± 2.01	5.87 ± 1.70	0.43	<0.001	<0.001
AC, ms	−4.34 ± 2.29	−4.69 ± 2.13	−6.27 ± 1.96	0.68	<0.001	<0.001
α_1	0.79 ± 0.26	0.72 ± 0.24	1.17 ± 0.25	0.44	<0.001	<0.001
α_2	0.93 ± 0.16	1.00 ± 0.21	1.18 ± 0.08	0.048	<0.001	<0.001
λ_{25s}	0.57 ± 0.18	0.48 ± 0.15	0.40 ± 0.08	<0.001	<0.001	<0.001
λ^2-slope	−0.21 ± 0.23	−0.13 ± 0.18	−0.02 ± 0.08	0.03	<0.001	<0.001

P< 0.05.

DC and AC. Indices such as LF/HF, and DFA α_1 and α_2 were also significantly decreased.

In the MSA patients, the pattern of changes in conventional HRV indices was similar to that observed in the CHF patients. While the decreased HRV in both MSA and CHF patients might reflect reduced vagal heart rate control, decreases in LF/HF and DFA α_1 were observed for both MSA, a disease with reported preganglionic sympathetic failure (Sone et al., 2005), and for CHF, a pathology associated with sympathetic overdrive (Packer, 1988; Clarke et al., 2008). In contrast, no decreases in SDNN and HF power, indices of reduced HRV, were observed in the PD patients, which might reflect relatively intact vagal heart rate control. However, decreases in LF/HF and DFA α_1 were also observed in PD, a disease with reported postganglionic sympathetic failure (Braune et al., 1998, 1999).

NON-GAUSSIAN AND INTERMITTENT PROPERTIES OF HRV

Figure 2 shows representative results of the multiscale PDF analysis for MSA, CHF, and PD patients (one patient from each group) and a healthy subject. As shown in **Figures 2M–P**, HRV data from the MSA and PD patients and the healthy subject yielded similar PDF curves at each scale. In contrast, recordings from the CHF patient yielded a PDF curve with a more tapered center and fatter tails at relatively smaller scales. This reflects intermittent large deviations or *bursts* observed at $s = 20$ s in CHF patients (**Figure 2G**), while this increased intermittency was not observed in the MSA and PD patients. In addition, as the scale s increases, deformation of PDFs toward a Gaussian distribution was clearly observed only in the CHF patient. The deformation process of the non-Gaussian PDF can be described by the relation between the non-Gaussianity index λ_s and scale s. As shown in **Figure 3**, the MSA and PD patient groups and the healthy subject groups showed nearly constant λ_s^2 values across a wide range of scales s, resulting in an almost zero value λ^2-slope. In contrast, the CHF patient group, particularly non-survivors, was characterized by almost linear increases in λ_s^2 as the log scale decreased from 200 to 20 s, similar to that observed for a cascade model of intermittent turbulence (**Figure 1B**). Consequently, the λ^2-slope for the CHF patients was significantly more negative than that for the healthy controls.

λ_{25s} for the MSA patients was slightly but significantly higher than that for healthy controls (**Table 3**), although the level was much lower than that for CHF non-survivors (**Table 5**). λ_{25s} for the PD patients failed to increase compared with that for healthy controls (**Table 4**). Both MSA and PD patients with sympathetic failure had λ^2-slopes of almost zero, which were not significantly different from those of healthy controls (**Tables 3** and **4**). Only CHF patients with known sympathetic overdrive had significantly negative λ^2-slopes (**Table 5**).

DISCUSSION

Long-term ambulatory HRV continues to attract clinical interest as a useful tool for risk stratification in AMI (Kleiger et al., 1987; Bigger et al., 1996; La Rovere et al., 1998; Schmidt et al., 1999; Huikuri et al., 2000; Bauer et al., 2006) and chronic heart failure (Ho et al., 1997; Nolan et al., 1998; Mäkikallio et al., 2001). Patients at higher mortality risk frequently have higher heart rates with reduced and less complex (or monotonic) HRV, and most indices used to characterize such HRV dynamics primarily reflect reduced or impaired vagal function (Lamm et al., 1999; Marine et al., 2002; Bauer et al., 2006). In contrast, few HRV indices are related to sympathetic function and their autonomic correlates and prognostic significance are still uncertain. For example, a decrease, but not the increase, in LF/HF, believed to reflect the sympathovagal balance (Pagani et al., 1986), is associated with increased mortality risk (Tsuji et al., 1994; Huikuri et al., 2000) in patients exhibiting sympathetic activation (Clarke et al., 2008). Similarly, a decrease in DFA α_1, known to be correlated with LF/HF and sensitive to changes in the sympathovagal balance (Huikuri et al., 2000), is associated with increased mortality risk (Huikuri et al., 2000; Mäkikallio et al., 2001). The present study further demonstrated that both of these indices are also decreased in MSA, a neurodegenerative disorder associated with preganglionic sympathetic failure

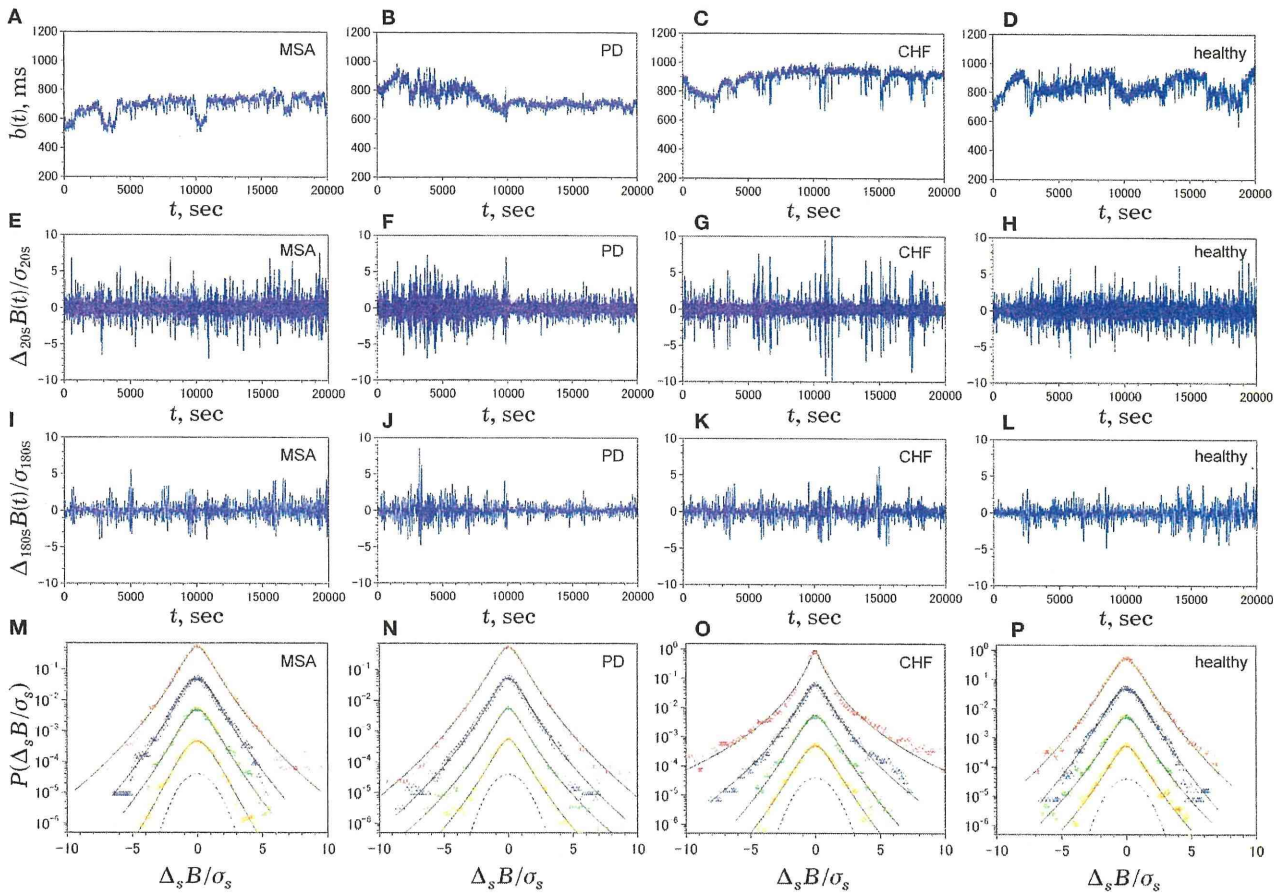

FIGURE 2 | Multiscale PDF characterization of heart rate variability. Illustrative examples of time series of NN intervals $b(t)$ **(A–D)**, time series of $\Delta_{20sB}(i)$ **(E–H)**, time series of $\Delta_{180sB}(i)$ **(I–L)**, and standardized PDFs (in logarithmic scale) of $\Delta_s B(i)$ for (from the top to bottom) $s = 20$, 60, 180, 300 s **(M–P)**, where σ_s denotes the SD of $\Delta_s B(i)$. In solid lines, we superimpose the PDF approximated by Castaing's model (Castaing et al., 1990). The panels on the leftmost side **(A,E,I,M)** are data for a 60-year-old male patient with multiple system atrophy (MSA). The panels on the left-of-center side **(B,F,J,N)** are data for a 68-year-old male patient with Parkinson disease (PD). The panels on the right-of-center side **(C,G,K,O)** are data for a 83-year-old female patient with congestive heart failure (CHF) who died 54 days after the measurement. The panels on the rightmost side **(D,H,L,P)** are data for a control subject (84-year-old male). For comparison, the dashed line denotes a Gaussian distribution. Note that, while the raw $b(t)$ for the patients looks much different from that for the control subject, the degrees of non-Gaussianity (i.e., the shapes of PDF) remain unaltered across scales for MSA and PD patients and the healthy control, except for those for the CHF patient at shorter scales **(G,O)**.

(Sone et al., 2005), and in PD, which is often accompanied by postganglionic sympathetic failure (Braune et al., 1998, 1999).

As a marker potentially related to sympathetic cardiac overdrive, we have recently introduced increased non-Gaussianity of HRV within LF and VLF ranges in patients with CHF and AMI (Kiyono et al., 2008; Hayano et al., 2011), cardiopathologies known to be associated with sympathetic overdrive (Packer, 1988; Cohn et al., 2000). In the present study, we further demonstrated that a marked increase in intermittent and non-Gaussian HRV was not observed in MSA and PD patients with sympathetic failure. We still have not determined why λ_{25s} for the MSA patients was slightly but significantly higher than that for healthy controls; this enhanced non-Gaussianity may be due to adrenergic stimulants administered to ameliorate severe orthostatic symptoms in the MSA patients. However, the scale-dependent increase in λ_s^2 with decreasing log scales mainly within the VLF range, leading to a markedly higher λ_{25s} in the CHF patients (**Table 5**), was not observed in MSA. Therefore, we suggest that the systematically increased non-Gaussianity of HRV within LF and VLF ranges could be a hallmark of sympathetic cardiac overdrive and that indices such as λ_{25s} and λ^2-slope could be used to measure the degree of sympathetic activation. Indeed, we recently observed decreased λ_{25s} in the AMI patients taking (anti-sympathetic) β-blockers (Hayano et al., 2011).

Using concepts developed in statistical and non-linear physics, it has been demonstrated that the healthy human heart rate fluctuates in a complex manner even under resting conditions, exhibiting fractal long-range correlations (Peng et al., 1993; Kobayashi and Musha, 1982) and multifractal properties (Ivanov et al., 1999; Amaral et al., 2001; Ching and Tang, 2007). Based on these findings, Liu and Hughson (2008) proposed an analogy between heart rate dynamics and hydrodynamic turbulence because a

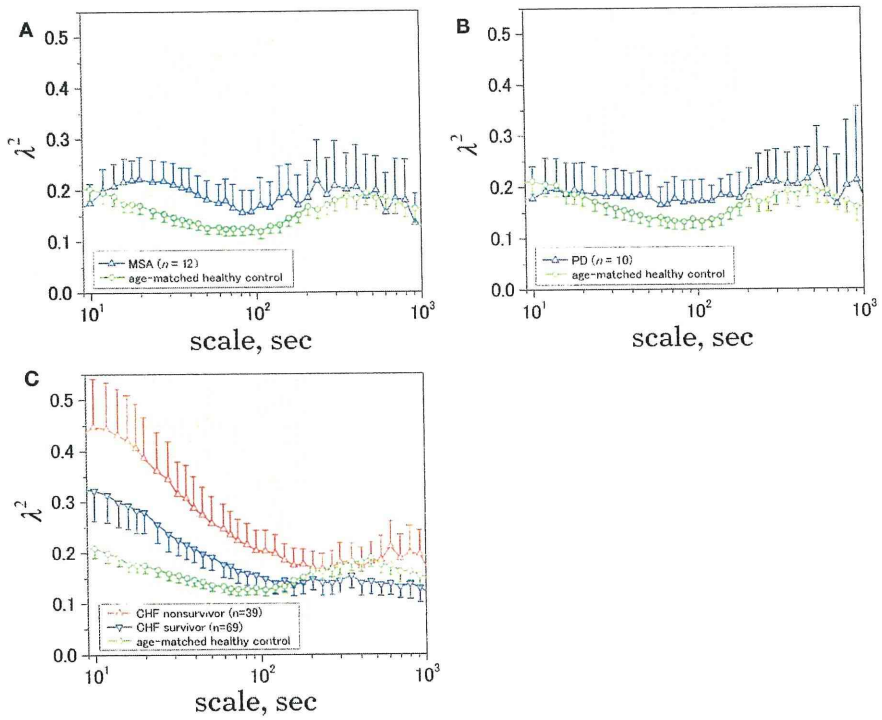

FIGURE 3 | Time-scale dependence of the non-Gaussianity index, λ^2. The results for **(A)** multiple system atrophy (MSA), **(B)** Parkinson disease (PD), and **(C)** congestive heart failure (CHF) patients, both for survivor (SV; $n = 69$) and non-survivor (NS; $n = 39$). Age-matched controls were selected from a database of healthy subjects. Error bars indicate 95%-confidence intervals of the group averages.

phenomenological model of hydrodynamic turbulence, called the multiplicative cascade model (Mandelbrot and Taylor, 1967), can also have multifractal properties. Using multiscale PDF analysis, we later demonstrated that the healthy human HRV does not show slow and gradual convergence to a Gaussian distribution (Kiyono et al., 2004; **Figure 3**), an important requirement of the multiplicative cascade model (**Figure 1B**). In contrast, the present study and previous work (Kiyono et al., 2008) suggest that HRV within LF and VLF ranges of CHF patients, especially non-survivors, is more compatible with the multiplicative cascade model.

The multiplicative (log-normal) cascade model used to generate fluctuations with intermittent bursts such as those shown in **Figure 1A** is given by

$$x_i = \xi_i \exp\left[\sum_{j=1}^{m} \omega^{(j)}\left(\left\lfloor \frac{j-1}{2^{m-j}} \right\rfloor\right)\right],$$

where ξ_i is Gaussian white noise with zero mean, $\omega^{(j)}(k)$ are independent Gaussian random variables with zero mean and constant variance, and $\lfloor \cdot \rfloor$ is the floor function (Kiyono et al., 2007). The m is the total number of cascade steps, yielding the total number of data points 2^m ($i = 1, \ldots, 2^m$). An essential part of the model is that ξ_i is modulated by multiplication of random (log-normal) weights $\exp[\omega^{(j)}(k)]$ ($k = 0, 1, \ldots, 2^j - 1$) at the j-th step every 2^{m-j} subintervals; therefore, large fluctuations are observed only when the momentary weights for (many) different steps with varying timescales are simultaneously large (refer to Figure 5 of Kiyono et al., 2007). Using multiscale PDF analysis, Kiyono et al. (2007) further showed that this model exhibits the scale dependence of a non-Gaussianity index in the form of $\lambda_s^2 \sim \ln s$ (**Figure 1B**).

The fact that heart rate dynamics of CHF patients with sympathetic activation exhibit a non-Gaussianity index which decays with scales within LF and VLF ranges suggests a sympathetic origin for HRV intermittency. In these scales (20–200 s), heart rate dynamics reflect cardiovascular regulation by neural, humoral, and thermal influences (Kitney and Rompelman, 1980). These subsystems are considered to be compensatory; therefore, it is likely that only simultaneous failure of all these subsystems operating at multiple timescales, compatible with the reciprocal of cascade steps "j" in the above example, could result in sympathetic overdrive, leading to large and intermittent heart rate deviations. We propose that such a *multiplicative picture* would provide a deeper physiological understanding of the nature of sympathetic function. In addition, it would provide a reason why methods requiring stationary, not intermittent, dynamics have not been successful in finding the sympathetic correlates of ambulatory HRV.

In the present study, we focused on daytime HRV for the following reasons. First, as reported in our previous study (Kiyono et al., 2005), there are large differences in non-Gaussianity and its scale dependence between day and night in healthy humans, presumably because of the difference in the sympathovagal balance. Second,

disorders of sleep and sleep breathing are common in MSA (Colosimo, 2011); therefore, incorporating nighttime data would inevitably introduce additional complexity. Third, one of our goals is to assess sympathetic activity, which is predominant during the day. Note that this shift from 24-h HRV to daytime HRV does not change our previous finding of the increased non-Gaussianity of low frequency HRV in CHF patients than in healthy controls (Kiyono et al., 2008).

In agreement with previous studies (Gurevich et al., 2004; Kuriyama et al., 2005), our MSA patients showed significantly decreased HRV, as evidenced by lower SDNN and HF power. This decrease is probably related to the known abnormalities in central vagal (Benarroch et al., 2006) and sympathetic function in these patients (Sone et al., 2005). On the other hand, changes in SDNN and HF power were not significant in PD patients, implying relatively intact vagal heart rate control despite the impaired peripheral, cardiac sympathetic function (Braune et al., 1998, 1999). Thus, analyses of ambulatory HRV may facilitate discriminative diagnosis between MSA and PD, particularly the difficult distinction between early stage PD and MSA with predominant Parkinsonian symptoms (Lipp et al., 2009).

ACKNOWLEDGMENTS

This research was supported in part by a Grant-in-Aid for Scientific Research (A) (23240094; to Yoshiharu Yamamoto) from the Japan Society for the Promotion of Science (JSPS) and by Core Research for Evolutional Science and Technology from Japan Science and Technology Agency (JST; to Yoshiharu Yamamoto).

REFERENCES

Amaral, L. A. N., Ivanov, P., Aoyagi, N., Hidaka, I., Tomono, S., Goldberger, A. L., Stanley, H. E., and Yamamoto, Y. (2001). Behavioral-independent features of complex heartbeat dynamics. *Phys. Rev. Lett.* 86, 6026–6029.

Bauer, A., Kantelhardt, J. W., Barthel, P., Schneider, R., Mäkikallio, T., Ulm, K., Hnatkova, K., Schömig, A., Huikuri, H. V., Bunde, A., Malik, M., and Schmidt, G. (2006). Deceleration capacity of heart rate as a predictor of mortality after myocardial infarction: cohort study. *Lancet* 367, 1674–1681.

Benarroch, E. E., Schmeichel, A. M., Sandroni, P., Low, P. A., and Parisi, J. E. (2006). Involvement of vagal autonomic nuclei in multiple system atrophy and Lewy body disease. *Neurology* 66, 378–383.

Bigger, J. T., Steinman, R. C., Rolnitzky, L. M., Fleiss, J. L., Albrecht, P., and Cohen, R. J. (1996). Power law behavior of RR-interval variability in healthy middle-aged persons, patients with recent acute myocardial infarction, and patients with heart transplants. *Circulation* 93, 2142–2151.

Braune, S., Reinhardt, M., Bathmann, J., Krause, T., Lehmann, M., and Lücking, C. H. (1998). Impaired cardiac uptake of meta-[123I]iodobenzylguanidine in Parkinson's disease with autonomic failure. *Acta Neurol. Scand.* 97, 307–314.

Braune, S., Reinhardt, M., Schnitzer, R., Riedel, A., and Lücking, C. H. (1999). Cardiac uptake of [123I]MIBG separates Parkinson's disease from multiple system atrophy. *Neurology* 53, 1020–1025.

Camm, A. J., Malik, M., Bigger, J. T. Jr., Breithardt, G., Cerutti, S., Cohen, R. J., Coumel, P., Fallen, E. L., Kleiger, R. E., Lombardi, F., Malliani, A., Moss, A. J., Rottman, J. N., Schmidt, G., Schwartz, P. J., and Singer, D. H. (1996). Heart rate variability: standards of measurement, physiological interpretation and clinical use. Task Force of the European Society of Cardiology and the North American Society of Pacing and Electrophysiology. *Circulation* 93, 1043–1065.

Castaing, B., Gagne, Y., and Hopfinger, E. (1990). Velocity probability density functions of high Reynolds number turbulence. *Physica D* 46, 177–200.

Ching, E. S. C., and Tsang, Y.-K. (2007). Multifractality and scale invariance in human heartbeat dynamics. *Phys. Rev. E Stat. Nonlin. Soft Matter Phys.* 76, 041910.

Ciarka, A., van de Borne, P., and Pathak, A. (2008). Myocardial infarction, heart failure and sympathetic nervous system activity: new pharmacological approaches that affect neurohumoral activation. *Expert Opin. Investig. Drugs* 17, 1315–1330.

Colosimo, C. (2011). Nonmotor presentations of multiple system atrophy. *Nat. Rev. Neurol.* 7, 295–298.

Efron, B., and Tibshirani, R. J. (1993). *An Introduction to the Bootstrap*. New York: Chapman & Hall.

Ghashghaie, S., Breymann, W., Peinke, J., Talkner, P., and Dodge, Y. (1996). Turbulent cascades in foreign exchange markets. *Nature* 381, 767–770.

Gilman, S., Wenning, G. K., Low, P. A., Brooks, D. J., Mathias, C. J., Trojanowski, J. Q., Wood, N. W., Colosimo, C., Dürr, A., Fowler, C. J., Kaufmann, H., Klockgether, T., Lees, A., Poewe, W., Quinn, N., Revesz, T., Robertson, D., Sandroni, P., Seppi, K., and Vidailhet, M. (2008). Second consensus statement on the diagnosis of multiple system atrophy. *Neurology* 71, 670–676.

Gurevich, T. Y., Groozman, G. B., Giladi, N., Drory, V. E., Hausdorff, J. M., and Korczyn, A. D. (2004). R-R interval variation in Parkinson's disease and multiple system atrophy. *Acta Neurol. Scand.* 109, 276–279.

Hayano, J., Kiyono, K., Struzik, Z. R., Yamamoto, Y., Watanabe, E., Stein, P. K., Watkins, L. L., Blumenthal, J. A., and Carney, R. M. (2011). Increased non-Gaussianity of heart rate variability predicts cardiac mortality after an acute myocardial infarction. *Front. Physiol.* 2:65. doi:10.3389/fphys.2011.00065

Ho, K. K. L., Moody, G. B., Peng, C.-K., Mietus, J. E., Larson, M. G., Levy, D., and Goldberger, A. L. (1997). Predicting survival in heart failure case and control subjects by use of fully automated methods for deriving nonlinear and conventional indices of heart rate dynamics. *Circulation* 96, 842–848.

Hughes, A. J., Daniel, S. E., Kilford, L., and Lees, A. J. (1992). Accuracy of clinical diagnosis of idiopathic Parkinson's disease: a clinico-pathological study of 100 cases. *J. Neurol. Neurosurg. Psychiatr.* 55, 181–184.

Huikuri, H. V., Mäkikallio, T. H., Peng, C.-K., Goldberger, A. L., Hintze, U., and Møller, M. (2000). Fractal correlation properties of R-R interval dynamics and mortality in patients with depressed left ventricular function after an acute myocardial infarction. *Circulation* 101, 47–53.

Huikuri, H. V., Perkiömäki, J. S., Maestri, R., and Pinna, G. D. (2009). Clinical impact of evaluation of cardiovascular control by novel methods of heart rate dynamics. *Philos. Transact. A Math. Phys. Eng. Sci.* 367, 1223–1238.

Ivanov, P. C., Amaral, L. A. N., Goldberger, A. L., Havlin, S., Rosenblum, M. G., Struzik, Z. R., and Stanley, H. E. (1999). Multifractality in human heart rate dynamics. *Nature* 399, 461–465.

Kitney, R. I., and Rompelman, O. (eds). (1980). *The Study of Heart-Rate Variability*. Oxford: Clarendon Press.

Kiyono, K., Hayano, J., Watanabe, E., Struzik, Z. R., and Yamamoto, Y. (2008). Non-Gaussian heart rate as an independent predictor of mortality in patients with chronic heart failure. *Heart Rhythm* 5, 261–268.

Kiyono, K., Struzik, Z. R., Aoyagi, N., Sakata, S., Hayano, J., and Yamamoto, Y. (2004). Critical scale invariance in a healthy human heart rate. *Phys. Rev. Lett.* 93, 178103.

Kiyono, K., Struzik, Z. R., Aoyagi, N., Togo, F., and Yamamoto, Y. (2005). Phase transition in a healthy human heart rate. *Phys. Rev. Lett.* 95, 058101.

Kiyono, K., Struzik, Z. R., and Yamamoto, Y. (2007). Estimator of a non-Gaussian parameter in multiplicative log-normal models. *Phys. Rev. E Stat. Nonlin. Soft Matter Phys.* 76, 041113.

Kleiger, R. E., Miller, J. P., Bigger, J. T., Moss, A. J., and The Multicenter Post-Infarction Research Group. (1987). Decreased heart rate variability and its association with increased mortality after acute myocardial infarction. *Am. J. Cardiol.* 59, 256–262.

Kuriyama, N., Mizuno, T., Iida, A., Watanabe, Y., and Nakagawa, M. (2005). Autonomic nervous evaluation in the early stages of olivopontocerebellar atrophy. *Auton. Neurosci.* 123, 87–93.

La Rovere, M. T., Bigger, J. T., Marcus, F. I., Mortara, A., and Schwartz, P. J. (1998). Baroreflex sensitivity and heart-rate variability in prediction of total cardiac mortality after myocardial infarction. *Lancet* 351, 478–484.

Lin, D., and Hughson, R. L. (2001). Modeling heart rate variability in healthy humans: a turbulence analogy. *Phys. Rev. Lett.* 86, 1650–1653.

Lipp, A., Sandroni, P., Ahlskog, J. E., Fealey, R. D., Kimpinski, K., Iodice, V., Gehrking, T. L., Weigand, S. D., Sletten, D. M., Gehrking, J. A., Nickander, K. K., Singer, W., Maraganore, D. M., Gilman, S., Wenning, G. K., Shults, C. W., and Low, P. A. (2009). Prospective differentiation of multiple system atrophy from Parkinson disease, with and without autonomic failure. *Arch. Neurol.* 66, 742–750.

Mäkikallio, T. H., Huikuri, H. V., Hintze, U., Videbaek, J., Mitrani, R. D., Castellanos, A., Myeburg, R. J., Møller, M., and Myerburg, R. J. (2001). Fractal analysis and time- and frequency-domain measures of heart rate variability as predictors of mortality in patients with heart failure. *Am. J. Cardiol.* 87, 178–182.

Marine, J. E., Watanabe, M. A., Smith, T. W., and Monahan, K. M. (2002). Effect of atropine on heart rate turbulence. *Am. J. Cardiol.* 89, 767–769.

McEwen, B. S. (1998). Protective and damaging effects of stress mediators. *N. Engl. J. Med.* 338, 171–179.

McEwen, B. S. (2007). Physiology and neurobiology of stress and adaptation: central role of the brain. *Physiol. Rev.* 87, 873–904.

Monin, A. S., and Yaglom, A. M. (1975). *Statistical Fluid Mechanics.* Cambridge, MA: MIT Press.

Nolan, J., Batin, P. D., Andrews, R., Lindsay, S. J., Brooksby, P., Mullen, M., Baig, W., Flapan, A. D., Cowley, A., Prescott, R. J., Neilson, J. M., and Fox, K. A. (1998). Prospective study of heart rate variability and mortality in chronic heart failure. Results of the United Kingdom heart failure evaluation and assessment of risk trial (UK-Heart). *Circulation* 98, 1510–1516.

Packer, M. (1988). Neurohormonal interactions and adaptations in congestive heart failure. *Circulation* 77, 721.

Pagani, M., Lombardi, F., Guzzetti, S., Rimoldi, O., Furlan, R., Pizzinelli, P., Sandrone, G., Malfatto, G., Dell'Orto, S., Piccaluga, E., Turiel, M., Baselli, G., Cerutti, S., and Malliani, A. (1986). Power spectral analysis of heart rate and arterial pressure variabilities as a marker of sympatho-vagal interaction in man and conscious dog. *Circ. Res.* 59, 178–193.

Peng, C. K., Havlin, S., Stanley, H. E., and Goldberger, A. L. (1995). Quantification of scaling exponents and crossover phenomena in nonstationary heartbeat time series. *Chaos* 5, 82–87.

Peng, C.-K., Mietus, J., Hausdorff, J. M., Havlin, S., Stanley, H. E., and Goldberger, A. L. (1993). Long-range anticorrelations and non-Gaussian behavior of the heartbeat. *Phys. Rev. Lett.* 70, 1343–1346.

Schmidt, G., Malik, M., Barthel, P., Schneider, R., Ulm, K., Rolnitzky, L., and Camm, A. J. (1999). Heart-rate turbulence after ventricular premature beats as a predictor of mortality after acute myocardial infarction. *Lancet* 353, 1390–1396.

Schwartz, P. J., Billman, G. E., and Stone, H. L. (1984). Autonomic mechanisms in ventricular fibrillation induced by myocardial ischemia during exercise in dogs with healed myocardial infarction. An experimental preparation for sudden cardiac death. *Circulation* 69, 790–800.

Sone, M., Yoshida, M., Hashizume, Y., Hishikawa, N., and Sobue, G. (2005). alpha-Synuclein-immunoreactive structure formation is enhanced in sympathetic ganglia of patients with multiple system atrophy. *Acta Neuropathol.* 110, 19–26.

Stefanova, N., Bücke, P., Duerr, S., and Wenning, G. K. (2009). Multiple system atrophy: an update. *Lancet Neurol.* 8, 1172–1178.

Tsuji, H., Venditti, F. J., Manders, E. S., Evans, J. C., Larson, M. G., Feldman, C. L., and Levy, D. (1994). Reduced heart rate variability and mortality risk in an elderly cohort. The Framingham Heart Study. *Circulation* 90, 878–883.

Wenning, G. K., Stefanova, N., Jellinger, K. A., Poewe, W., and Schlossmacher, M. G. (2008). Multiple system atrophy: a primary oligodendrogliopathy. *Ann. Neurol.* 64, 239–246.

Yamamoto, Y., and Hughson, R. L. (1994). On the fractal nature of heart rate variability in humans: effects of data length and beta-adrenergic blockade. *Am. J. Physiol.* 266, R40–R49.

Conflict of Interest Statement: The authors declare that the research was conducted in the absence of any commercial or financial relationships that could be construed as a potential conflict of interest.

Received: 09 December 2011; accepted: 07 February 2012; published online: 22 February 2012.

Citation: Kiyono K, Hayano J, Kwak S, Watanabe E and Yamamoto Y (2012) Non-Gaussianity of low frequency heart rate variability and sympathetic activation: lack of increases in multiple system atrophy and Parkinson disease. Front. Physio. 3:34. doi: 10.3389/fphys.2012.00034

This article was submitted to Frontiers in Computational Physiology and Medicine, a specialty of Frontiers in Physiology.

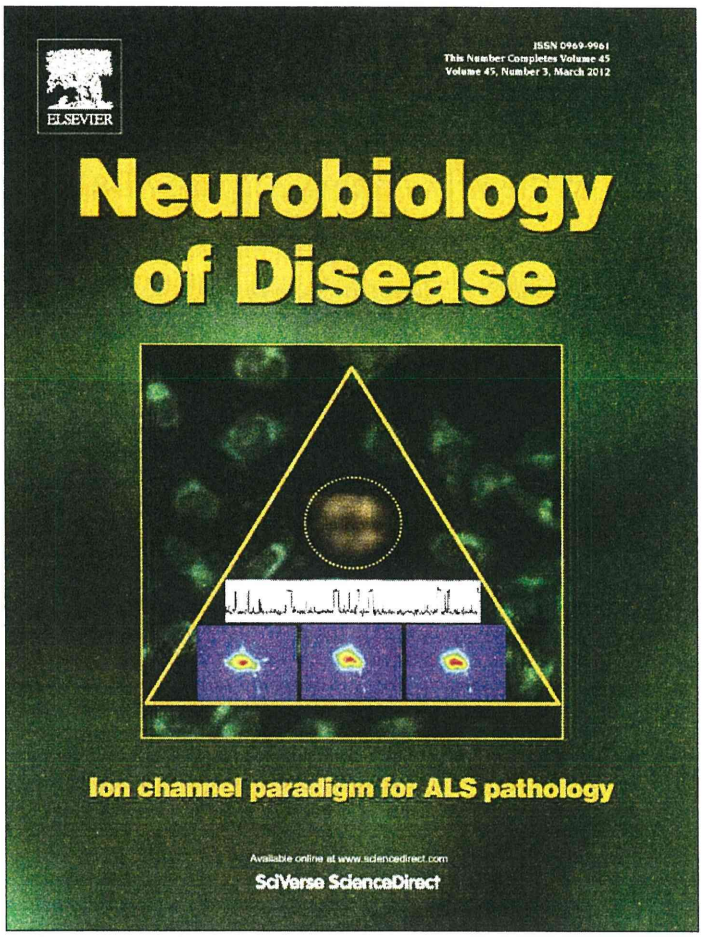

Neurobiology of Disease 45 (2012) 1121–1128

Contents lists available at SciVerse ScienceDirect

Neurobiology of Disease

journal homepage: www.elsevier.com/locate/ynbdi

Profound downregulation of the RNA editing enzyme ADAR2 in ALS spinal motor neurons

Takuto Hideyama [a,b,c], Takenari Yamashita [a,b], Hitoshi Aizawa [d], Shoji Tsuji [b], Akiyoshi Kakita [e], Hitoshi Takahashi [e], Shin Kwak [a,b,*]

[a] CREST, Japan Science and Technology Agency, University of Tokyo, 7-3-1 Hongo, Bunkyo-ku, Tokyo 113-8655, Japan
[b] Department of Neurology, Graduate School of Medicine, University of Tokyo, 7-3-1 Hongo, Bunkyo-ku, Tokyo 113-8655, Japan
[c] Division for Health Promotion, University of Tokyo, 7-3-1 Hongo, Bunkyo-ku, Tokyo 113-8655, Japan
[d] Department of Neurology, National Hospital Organization Tokyo National Hospital, 3-1-1 Takeoka Kiyose-shi, Tokyo 204-8585, Japan
[e] Department of Pathology, Brain Research Institute, Niigata University, 1-757 Asahimachi, Chuo-ku, Niigata 951-8585, Japan

ARTICLE INFO

Article history:
Received 26 October 2011
Revised 8 December 2011
Accepted 17 December 2011
Available online 28 December 2011

Keywords:
RNA editing
ADAR2 (adenosine deaminase acting on RNA 2)
ALS (amyotrophic lateral sclerosis)
GluA2
AMPA
Neuronal death

ABSTRACT

Amyotrophic lateral sclerosis (ALS) is the most common adult-onset fatal motor neuron disease. In spinal motor neurons of patients with sporadic ALS, normal RNA editing of GluA2, a subunit of the L-α-amino-3-hydroxy-5-methyl-4-isoxazolepropionic acid (AMPA) receptor, is inefficient. Adenosine deaminase acting on RNA 2 (ADAR2) specifically mediates RNA editing at the glutamine/arginine (Q/R) site of GluA2 and motor neurons expressing Q/R site-unedited GluA2 undergo slow death in conditional ADAR2 knockout mice. Therefore, investigation into whether inefficient ADAR2-mediated GluA2 Q/R site-editing occurs universally in motor neurons of patients with ALS would provide insight into the pathogenesis of ALS. We analyzed the extents of GluA2 Q/R site-editing in an individual laser-captured motor neuron of 29 ALS patients compared with those of normal and disease control subjects. In addition, we analyzed the enzymatic activity of three members of the ADAR family (ADAR1, ADAR2 and ADAR3) in ALS motor neurons expressing unedited GluA2 mRNA and those expressing only edited GluA2 mRNA. Q/R site-unedited GluA2 mRNA was expressed in a significant proportion of motor neurons from all of the ALS cases examined. Conversely, motor neurons of the normal and disease control subjects expressed only edited GluA2 mRNA. ADAR2, but not ADAR1 or ADAR3, was significantly downregulated in all the motor neurons of ALS patients, more extensively in those expressing Q/R site-unedited GluA2 mRNA than those expressing only Q/R site-edited GluA2 mRNA. These results indicate that ADAR2 downregulation is a profound pathological change relevant to death of motor neurons in ALS.

Introduction

Amyotrophic lateral sclerosis (ALS) is the most common adult-onset fatal motor neuron disease with unknown etiology. In spinal motor neurons of patients with ALS, normal RNA editing of GluA2, a subunit of the L-α-amino-3-hydroxy-5-methyl-4-isoxazolepropionic acid (AMPA) receptor, is inefficient (Kawahara et al., 2004a; Kwak and Kawahara, 2005; Takuma et al., 1999). This is in marked contrast to the fact that all GluA2 mRNA expressed in the spinal motor neurons was edited in control subjects (Kawahara et al., 2004a; Kwak and Kawahara, 2005; Takuma et al., 1999), in patients with motor neuron diseases other than sporadic ALS (Kawahara et al., 2006; Kwak and Kawahara, 2005) and in dying neurons in neurodegenerative diseases, including degenerating Purkinje cells of patients with spinocerebellar degeneration (Akbarian et al., 1995; Kawahara et al., 2004a; Suzuki et al., 2003).

Conversion of glutamine (Q) to arginine (R) at the Q/R site of GluA2 affects multiple AMPA receptor properties, including Ca^{2+} permeability of receptor-coupled ion channels, receptor trafficking, and assembly of receptor subunits (Burnashev et al., 1992; Greger et al., 2003; Greger et al., 2002; Sommer et al., 1991). In the GluA2 pre-mRNA, the adenosine coding for the Q/R site is converted to inosine (A-to-I conversion) by adenosine deaminase acting on RNA 2 (ADAR2) (Higuchi et al., 1993; Melcher et al., 1996), and inosine is read as guanosine during translation, thereby converting the genomic

Abbreviations: ALS, amyotrophic lateral sclerosis; ADAR2, adenosine deaminase acting on RNA 2; AH, anterior horn; AMPA, L-α-amino-3-hydroxy-5-methyl-4-isoxazolepropionic acid; BLCAP, bladder cancer associated protein; CYFIP2, cytoplasmic fragile X mental retardation protein interacting protein 2; GluA2, AMPA receptor subunit 2; MSA, multiple system atrophy; PBP, progressive bulbar palsy; PH, posterior horn; Q/R, glutamine/arginine; RT-PCR, reverse transcription polymerase chain reaction.

* Corresponding author at: Department of Neurology, Graduate School of Medicine, University of Tokyo, 7-3-1 Hongo, Bunkyo-ku, Tokyo 113-8655, Japan. Fax: +81 3 5800 6548.
E-mail address: kwak-tky@umin.ac.jp (S. Kwak).

Available online on ScienceDirect (www.sciencedirect.com).

0969-9961/$ – see front matter © 2011 Elsevier Inc. All rights reserved.
doi:10.1016/j.nbd.2011.12.033

Table 1
Profile of the cases with sporadic ALS.

Individual	Age at onset (year)	Clinical type of ALS	Duration of illness	Initial symptom
A1	77	Classic	2 y	U/E
A2	60	Classic	2 y 3 mo	U/E
A3	39	Classic	13 y	U/E, L/E
A4	77	Classic	1 y 7 mo	L/E
A5	69	Classic	2 y	U/E
A6	31	Classic	5 y	U/E
A7	57	Classic	1 y 9 mo	U/E
A8	72	Classic	5 y 3 mo	U/E
A9	67	Classic	2 y	U/E
A10	54	Classic	3 y	U/E
A11	58	Classic	3 y	U/E
A12	42	Classic	6 mo	U/E, L/E
A13	64	Classic	7 mo	U/E
A14	70	Classic	1 y 3 mo	U/E, L/E
A15	70	Classic	4 y	U/E
A16	71	Classic	2 y 9 mo	U/E
A17	80	Classic	2 y	U/E
A18	56	Classic	5y4 mo	U/E
A19	22	Baso	8 mo	U/E
A20	39	PBP	1 y 4 mo	Bulbar
A21	77	PBP	2 y	Bulbar
A22	78	PBP	1 y 4 mo	Bulbar
A23	85	PBP	1 y 8 mo	Bulbar
A24	43	PBP	1 y 5 mo	Bulbar, U/E
A25	70	PBP	4 y	Bulbar
A26	58	ALS-D	10 mo	U/E, L/E
A27	76	ALS-D	2 y	U/E
A28	67	PBP	4 y 5 mo	Bulbar
A29	75	PBP	2 y 6 mo	Bulbar

Classic: limb-onset classical ALS, PBP: progressive bulbar palsy, ALS-D: ALS with dementia, Baso: ALS with basophilic inclusion body, y: year, mo: month, Bulbar: dysarthria and/or dysphagia, U/E: weakness and/or amyotrophy in upper extremities, L/E: weakness and/or amyotrophy in lower extremities.

Q codon (CAG) to an R codon (CGG) at the Q/R site of GluA2. Because A-to-I conversion at the GluA2 Q/R site occurs in all GluA2 expressed in neurons, only Q/R site-edited GluA2 is expressed in virtually all neurons in the mammalian brain (Seeburg, 2002). Failure of Q-to-R conversion at this site produces Ca^{2+}-permeable AMPA receptors, resulting in increased excitation of neurons, which has been shown to culminate in fatal status epilepticus in mice (Brusa et al., 1995; Feldmeyer et al., 1999; Higuchi et al., 2000). Moreover, ADAR2-deficient motor neurons undergo slow death due to failure of GluA2 Q/R site-editing with expression of unedited GluA2 in conditional ADAR2 knockout (ADAR2$^{flox/flox}$VAChT-Cre.Fast or AR2) mice (Hideyama et al., 2010). Because A-to-I nucleotide conversion in the pre-mRNA for the GluA2 Q/R site is critical to survival of motor neurons, we investigated whether the expression of unedited GluA2 with a reduction of ADAR2 occurs in motor neurons of patients with sporadic ALS irrespective of the phenotype.

Materials and methods

All studies were carried out in accordance with the Declaration of Helsinki, and the Ethics Committee of the University of Tokyo approved the experimental procedures used.

Study population and spinal cord and brain tissue samples

Frozen spinal cords from pathologically proven patients with ALS (n = 29; age 23–87 years) were used in this study (Table 1). Spinal cords from patients with multiple system atrophy (MSA) (n = 5; age 65–78 years) and from control subjects (n = 12; age 27–82) were used as disease and normal controls, respectively (Table 2). The ALS group included classical limb-onset ALS, progressive bulbar palsy (PBP), ALS with long clinical course, ALS with basophilic inclusion body, and ALS with dementia. All patients were clinically examined by neurologists prior to death and none had relatives with ALS. Previously reported cases (Kawahara et al., 2004a) were included in this study, but we obtained additional samples from these cases. Spinal cord tissues were rapidly frozen on dry ice immediately after removal at autopsy and were kept at −80 °C until use. Written informed consent was obtained from all of the subjects prior to death or from their relatives.

Samples of the anterior horn (AH), posterior horn (PH) and white matter (SpW) of the spinal cord were obtained by dissecting frozen axial spinal cord sections under a binocular microscope within a freezing chamber. In addition, single motor neurons were dissected with a laser microdissector (Leica AS LMD, Leica Microsystems) as previously described (Kawahara et al., 2004a; Kawahara et al., 2003b; Takuma et al., 1999). Total RNA was isolated from dissected tissues, and first-strand cDNA was synthesized and treated with DNA-ase I (Invitrogen) as previously described (Kawahara et al., 2003a; Kawahara et al., 2003b).

Analysis for editing efficiency at A–I sites

Editing efficiencies at the Q/R sites in GluA2 mRNA were calculated by quantitative analyses of the digests of RT-PCR products with *BbvI* as previously described (Kawahara et al., 2004a; Kawahara et al., 2003a; Kawahara et al., 2003b; Takuma et al., 1999). In brief, 2 μl of cDNA was subjected to first PCR in duplicate in a reaction mixture of 50 μl containing 200 mM each primer, 1 mM dNTP Mix (Eppendorf AG), 5 μl of 10× PCR buffer and 1 μl of Advantage 2 Polymerase mix (BD Biosciences Clontech). The PCR amplification began with a 1-min denaturation step at 95 °C, followed by 40 cycles of denaturation at 95 °C for 10 s, annealing at 58 °C for 30 s and extension at 68 °C for 40 s. Nested PCR was conducted on 2 μl of the first PCR product under the same conditions with the exception of the annealing temperature (56 °C). Primer pairs used for each PCR were listed in Table S1. After gel purification using the Zymoclean Gel DNA Recovery Kit according to the manufacturer's protocol (Zymo Research), an aliquot (0.5 mg) was incubated with *BbvI* (New England BioLabs) at 37 °C for 12 h. The PCR products originating from Q/R site-edited GluA2 mRNA had one intrinsic restriction enzyme recognition site, whereas those originating from unedited mRNA had an additional recognition site. Thus, restriction digestion of the PCR products originating from edited GluA2 mRNA should produce different numbers of fragments (two bands at 116- and 66-bp) from those originating from unedited GluA2 mRNA (three bands at 35-, 81- and 66-bp). As the 66-bp band would originate from both edited and unedited mRNA, but the 116-bp band would originate from only edited mRNA, we

Table 2
Profile of the cases with sporadic ALS, control, and disease control (MSA).

Cases	Sporadic ALS				Control	MSA
	Classic	Baso	PBP	ALS-D		
	n = 18	n = 1	n = 8	n = 2	n = 12	n = 5
Age at onset (year) mean ± SD (range)	61.9 ± 13.7 (31–80)	22	66.8 ± 16.8 (41–87)	67.0 (58–76)	52.4 ± 18.0 (27–82)	71.6 ± 5.5 (65–78)
Duration of illness (month) mean ± SD (range)	38.2 ± 34.2 (6–156)*1	8	31.8 ± 12.5 (16–53)	17 (10–24)		

*1; with long duration (1 case): 156-mo, Classic: classical limb-onset ALS; PBP: progressive bulbar palsy; ALS-D: ALS with dementia; Baso: ALS with basophilic inclusion body; Control: neurologically free control subjects; MSA: multiple system atrophy. Please refer to Table 1 for a more detailed profile of the cases with sporadic ALS.

quantified the molarity of the 116- and 66-bp bands using the 2100 Bioanalyzer (Agilent Technologies) and calculated the editing efficiency as the ratio of the former to the latter for each sample (Supplementary Table 1).

With similar methods, we calculated the editing efficiencies at the Q/R sites in GluR6 mRNA and in GluA2 pre-mRNA, the R/G site in GluA2 mRNA, and the K/E sites in cytoplasmic fragile X mental retardation protein interacting protein 2 (CYFIP2) mRNA and pre-mRNA (Supplementary Table 1) (Kawahara et al., 2004a; Kawahara et al., 2003a; Kawahara et al., 2003b; Kwak et al., 2008; Nishimoto et al., 2008; Paschen et al., 1994; Takuma et al., 1999). Following restriction enzymes were used for restriction digestion of the respective A-to-I sites; *BbvI* for the Q/R sites, *NlaIV* (New England BioLabs) for the R/G sites, and *MseI* (New England BioLabs) for the K/E site. Primer pairs used for each PCR and sizes of restriction digests of PCR products were indicated in Supplementary Table 1.

Quantitative PCR

The expression levels of ADAR1, ADAR2, ADAR3, GluA2 and β-actin mRNAs were measured using the LightCycler system (Roche Diagnostics, Indianapolis, IN) (Kawahara et al., 2004a; Kawahara et al., 2003a; Takuma et al., 1999). To prepare an internal standard for quantitative PCR, gene-specific PCR products of approximately 1 kb in length were amplified from human cerebellar cDNA with the same primer pairs as previously reported (Supplementary Table 2) (Kawahara et al., 2004a; Kawahara et al., 2003a; Takuma et al., 1999). Each cDNA sample was amplified in a reaction mixture (20 ml total volume) composed of 10 μl of 2× LightCycler 480 Probes Master Roche (Roche Diagnostics), 0.5 mM of each primer set and 0.1 mM probes (Universal Probe Library Set, Human, Roche Diagnostics) (Supplementary Table 3).

DNA sequence

Editing efficiency at the Y/C site in mRNA of bladder cancer associated protein (BLCAP) was evaluated by sequencing the PCR products with a 3100 Genetic Analyzer sequencer (Applied Biosystems, Foster City, CA) (Supplementary Table 1).

Statistical analysis

Differences and correlations between two groups were evaluated using Mann–Whitney *U*-test with SPSS software (version 15; SPSS Inc., Chicago, IL) and Pearson product-moment correlation coefficient with GraphPad Prism version 5 (GraphPad Software, Inc., La Jolla, CA), respectively. Moreover, differences between three groups were evaluated using repeated ANOVA with GraphPad Prism version 5. Differences were considered statistically significant with $p<0.05$ and highly significant with $p<0.01$.

Results

Inefficient GluA2 editing in motor neurons is a universal molecular abnormality in patients with sporadic ALS

We analyzed the extent of GluA2 Q/R site-editing in spinal cord and motor neuron lysates from 29 cases of pathologically proven sporadic ALS of various phenotypes (Table 1). Efficiency of RNA editing at the GluA2 Q/R site in the anterior horn (AH) was nearly 100% in the control subjects, whereas efficiency was significantly lower in all of the ALS cases examined (Fig. 1A). To test whether unedited GluA2 mRNA was universally expressed in motor neurons in ALS cases, we examined the extent of GluA2 Q/R site-editing in lysates of motor neurons. Reverse transcription polymerase chain reaction (RT-PCR) products for GluA2 mRNA were not always yielded from lysates of a single motor neuron and approximately one third of the lysates yielded amplicons for GluA2 mRNA. When we could not effectively amplify RT-PCR products from any of the lysates of a single motor neuron in a case, we used lysates of 30 motor neurons dissected from the same case. We dissected more than 10,000 motor neurons, including 500 motor neurons of control subjects, 600 motor neurons of patients with MSA and 1270 motor neurons of patients with ALS. These lysates except those of 100 motor neurons from two ALS case (A28, A29) yielded GluA2 RT-PCR amplicons. The number of motor neurons examined and the mean editing efficiency in each case were shown in Supplementary Table 1. We found that at least one motor neuron in each of the 27 ALS cases expressed detectable amounts of unedited GluA2 mRNA. The proportion of unedited GluA2 varied among motor neurons in each ALS case, ranging from 0% to 100%. Conversely, all of the motor neurons from control subjects and patients with MSA expressed only edited GluA2 mRNA (Fig. 1B and Supplementary Table 1).

ADAR2 is downregulated in all the motor neurons including apparently normal motor neurons that express only edited GluA2

In the AH, the expression level of ADAR2 mRNA relative to GluA2 mRNA in ALS cases was decreased to less than one third of that in control cases. In contrast, expression levels in the PH and the SpW of the spinal cord of ALS cases were not different from those of the control cases (Fig. 2A). After examining whether unedited GluA2 mRNA was contained in each single motor neuron lysate, we pooled cDNA from 100 single motor neuron lysates of four ALS cases that contained only edited GluA2 mRNA (ALS^{edit}). We pooled together cDNA from 47 motor neurons that expressed unedited GluA2 mRNA into a sample called ALS^{uned} (Fig. 3). In addition, we obtained lysates of 100 or 30 motor neurons from control subjects and MSA cases. We analyzed the expression level of ADAR2 mRNA in these lysates relative to GluA2 mRNA (Fig. 2B) and β-actin mRNA (Fig. 2C). Both analyses demonstrated that the motor neurons of ALS patients expressed significantly lower amounts of ADAR2 mRNA than those of the control subjects or patients with MSA. Notably, the expression level of ADAR2 mRNA was much lower for ALS^{uned} than for ALS^{edit} (Figs. 2B and C).

Next, we examined the efficiencies of A-to-I conversion at ADAR2-mediated conversion positions. A-to-I conversion at the Q/R site of GluA2 pre-mRNA and the K/E site in CYFIP2 are specifically mediated by ADAR2 (Kwak et al., 2008; Nishimoto et al., 2008; Riedmann et al., 2008), and A-to-I conversion at the Q/R site of GluR6 is partially mediated by ADAR2 (Higuchi et al., 2000; Paschen et al., 1994). The editing efficiencies at these sites in lysates were lower in ALS cases than in control cases, although the difference in the efficiency of GluR6 Q/R site-editing between ALS and control cases did not reach statistical significance (Figs. 2D–F). Furthermore, efficiencies of editing at these sites were significantly correlated with the efficiency of GluA2 Q/R site-editing (Supplementary Figs. 1A and B). These results indicate that ADAR2 activity is significantly decreased in ALS motor neurons.

ADAR1 and ADAR3, other members of the ADAR family, play no role in ALS pathogenesis

There are three members of the ADAR family, including ADAR1, ADAR2 and ADAR3. ADAR1 catalyzes A-to-I editing in vivo with different but overlapping site-selectivity from ADAR2 (Levanon et al., 2005; Nishimoto et al., 2008; Wang et al., 2004), whereas editing activity has not been demonstrated for ADAR3 that predominantly localizes in brains (Chen et al., 2000). The expression levels of ADAR1 mRNA in lysates of ALS motor neurons (both ALS^{edit} and ALS^{uned}) were similar to or even higher than those in lysates of control motor neurons (Fig. 4A). In addition, efficiencies of ADAR1-

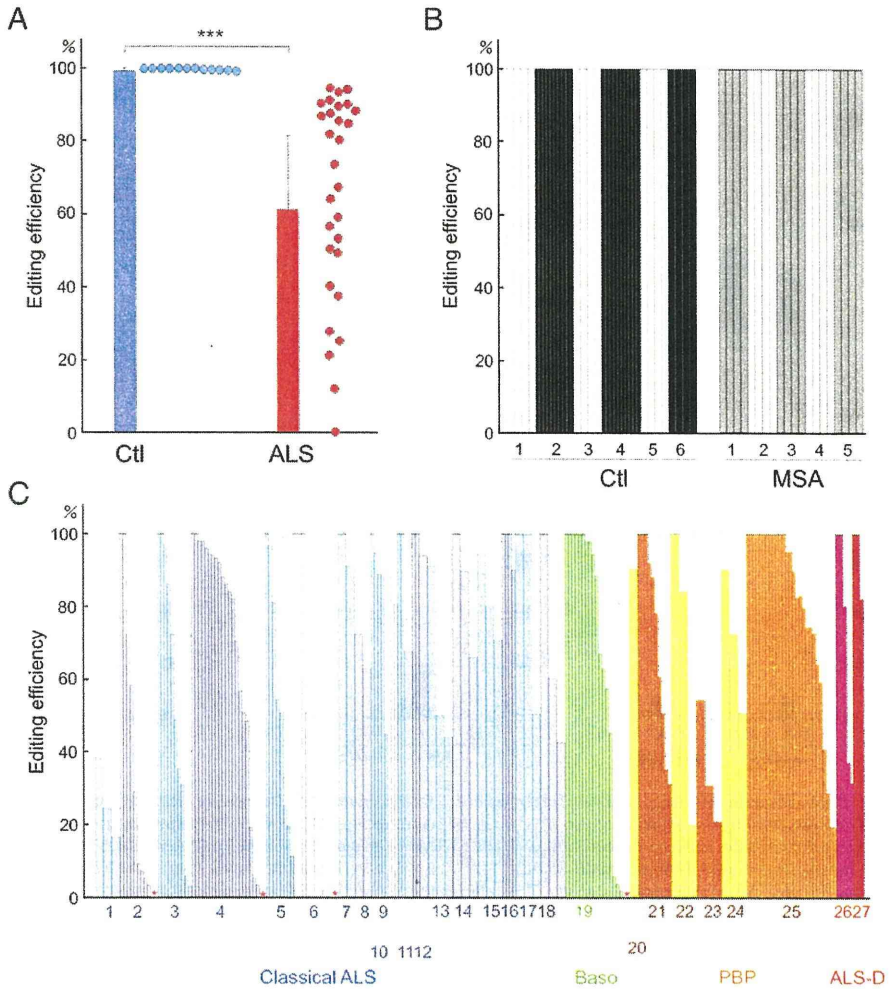

Fig. 1. Reduction of GluA2 Q/R site-editing in ALS motor neurons. (A) Editing efficiencies at the GluA2 Q/R site in anterior horn (AH) lysates of spinal cord from sporadic ALS patients (ALS) and control subjects (Ctl). Editing efficiencies for the ALS group (ALS, n = 29) was significantly lower than that of the control group (Ctl, n = 12) (61.0% ± 22.7% vs. 99.4% ± 0.7%; ***$p < 0.001$). Each circle represents the extent of GluA2 Q/R site-editing in each ALS case (red) or control case (blue), illustrating that values representing editing efficiency were less than 100% in all ALS cases, whereas those in the control subjects were approximately 100%. Columns and bars represent the mean ± SEM. (B and C) Extents of GluA2 Q/R site-editing in motor neuron lysates. Each narrow bar represents the editing efficiency in the lysate of one motor neuron, and each wide bar represents the editing efficiency in the lysate of 30 motor neurons. The results from the lysates of an individual case are shown in the same color. Editing efficiency was 100% in all motor neurons from all control subjects and patients with multiple system atrophy (MSA). Note that the extent of editing was less than 100% in at least one motor neuron of all 27 ALS cases examined, regardless of the clinical phenotype. Red asterisks indicate lysates showing 0% editing efficiency. Classical ALS: limb-onset ALS (blue); Baso: ALS with basophilic inclusion body (green); PBP: progressive bulbar palsy (orange); ALS-D: ALS with dementia (red).

mediated A-to-I conversion at the R/G site of GluA2 mRNA (Wang et al., 2004) and the Y/C site of bladder cancer associated protein (BLCAP) mRNA (Kwak et al., 2008; Nishimoto et al., 2008) in the ALS AH lysates did not differ from those in the control AH lysates (Figs. 4B and C and Supplementary Fig. 1C). Finally, ADAR3 mRNA expression level in the lysate of the ALS AH did not differ from that of the control AH (Supplementary Fig. 1D).

Discussion

The consistent results obtained from a large number of single motor neurons derived from a considerable number of ALS cases clearly demonstrate that inefficient GluA2 Q/R site-editing is a disease-specific molecular abnormality observed among sporadic ALS patients with different clinical manifestations, including classical limb-onset ALS, progressive bulbar palsy and ALS with dementia. GluA2 Q/R site-editing is fully preserved throughout life from the embryonic stage in mammalian brains (Burnashev et al., 1992; Nutt and Kamboj, 1994), including human brains (Kawahara et al., 2004b). A-to-I conversion at the GluA2 Q/R site is specifically mediated by ADAR2 (Higuchi et al., 2000), and motor neurons deficient in ADAR2 undergo slow death specifically due to a failure to edit this site, as observed in conditional ADAR2 knockout (AR2) mice (Hideyama et al., 2010). Expression of unedited GluA2 is also toxic in cultured cells (Mahajan and Ziff, 2007). Therefore, inefficient GluA2 Q/R site-editing is likely a common molecular abnormality and one cause of motor neuron death in ALS. Notably, the present study demonstrated that Q/R site-unedited GluA2 mRNA was expressed in motor neurons of two patients with ALS with dementia as occurred in patients with other clinical phenotypes of sporadic ALS. Based on the recent observation that ALS is not infrequently associated with the pathology in fronto-temporal lobar degeneration with ubiquitin-immunoreactive inclusion bodies (FTLD-U) and that degenerating neurons in both patients with ALS and those with FTLD-U exhibit TDP-43 pathology, it is believed that there is a common pathogenic mechanism between ALS and FTLD-U (Cairns et al., 2007). The present result is in agreement with this concept and lends support to the hypothesis that inefficient GluA2 Q/R site-

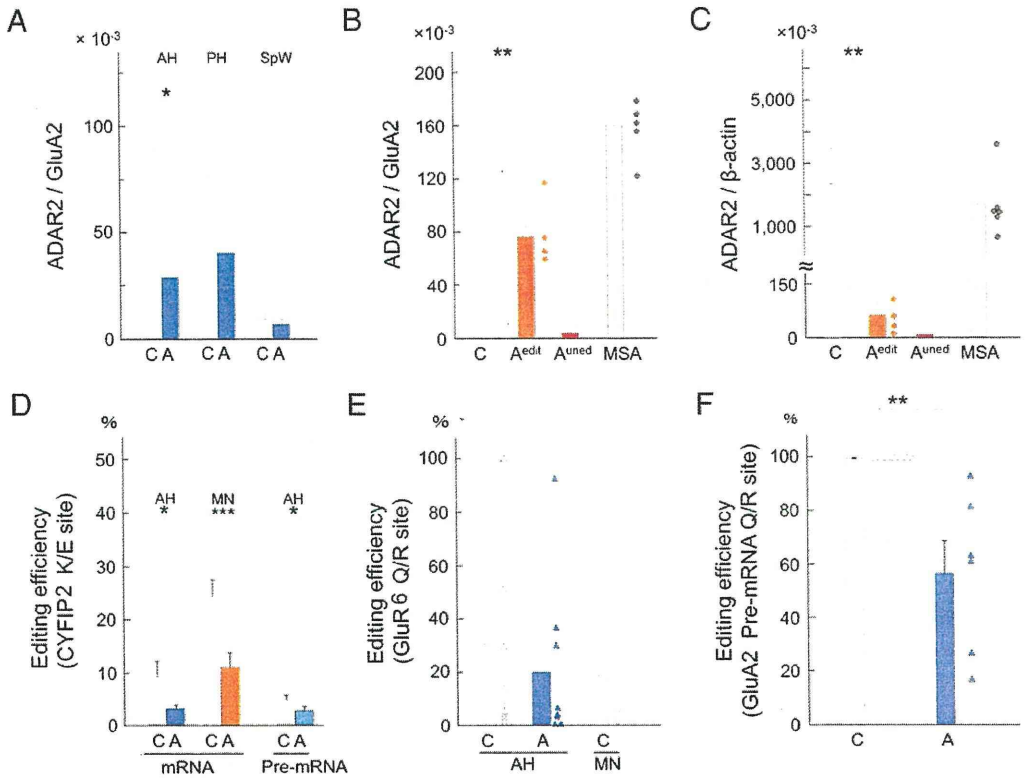

Fig. 2. Downregulation of ADAR2 mRNA and editing efficiency of ADAR2 substrates in ALS motor neurons. (A) The relative abundance of ADAR2 mRNA in the GluA2 mRNA base in the spinal cord anterior horn (AH) was significantly less in the ALS group (A) than in the control group (C) (*$p<0.05$). In contrast, relative abundance in the posterior horn (PH) or white matter (SpW) of the spinal cord did not differ between the two groups. (B and C) Relative abundance of ADAR2 mRNA in lysates of motor neurons in the GluA2 mRNA base (B) and β-actin mRNA base (C). The expression level of ADAR2 mRNA in ALS^{edit} (A^{edit}; $n=4$) was significantly lower than in the lysates of motor neurons of control subjects (C; $n=4$; **$p<0.02$), and that in ALS^{uned} (A^{uned}) was much lower than in A^{edit}. On the contrary, ADAR2 mRNA level in the MSA group did not differ from the C group. (D) Editing efficiency at the K/E site of CYFIP2 mRNA in lysates of AH (*$p<0.03$) and motor neurons (MN) (***$p<0.005$) and editing efficiency of CYFIP2 pre-mRNA in the AH (*$p<0.02$) were significantly lower in the ALS group (A) than in the control group (C). (E) Editing efficiency at the Q/R site of GluR6 mRNA was lower in the ALS AH than in the control AH, although this difference was not statistically significant. Editing efficiency at the GluR6 Q/R site was not significantly different between AH and the lysate of 100 MN from control spinal cord. (F) Editing efficiency at the Q/R site of GluA2 pre-mRNA in the AH lysates from the ALS group was lower than that of the lysates of the control group (**$p<0.01$). Columns and bars represent mean ± SEM. Each triangle represents a value for the AH lysate, and each circle represents a value for the MN lysate from a single case. C: Lysate of 100 motor neurons from control subjects ($n=4$). A^{edit}: lysate of 100 motor neurons expressing only Q/R site-edited GluA2 mRNA from ALS patients. A^{uned}: lysate of 47 motor neurons expressing Q/R site-unedited GluA2 mRNA from ALS patients. MSA: lysate of 30 motor neurons from the patients with multiple system atrophy ($n=6$).

editing is a common death-causing molecular abnormality in sporadic ALS.

Of the three members of the ADAR family, only ADAR2 was downregulated in ALS motor neurons. Although ADAR1 catalyzes A-to-I conversions that are critical during embryogenesis (XuFeng et al., 2009) and ADAR3 is predominantly localized in the central nervous system (Chen et al., 2000), neither ADAR1 nor ADAR3 participates in the inefficient GluA2 Q/R site-editing in ALS motor neurons. In addition, ADAR2 was downregulated in all ALS motor neurons, even in those motor neurons expressing only edited GluA2 (ALS^{edit}) and more extensively in those motor neurons expressing unedited GluA2 (ALS^{uned}), indicating profound downregulation of ADAR2 associated with sporadic ALS. Deficient ADAR2 induces death of motor neurons via failure to edit the GluA2 Q/R site, and expression of edited GluA2 by genetic engineering of the endogenous GluA2 gene rescues motor neurons lacking ADAR2 from death in AR2 mice (Hideyama et al., 2010). Investigations on the conditional ADAR2 knockout mice in which one ADAR2 gene allele was ablated in motor neurons (HeteroAR2; $ADAR2^{flox/+}$/VAChT-Cre.Fast) demonstrated that the motor neurons with reduced ADAR2 expressed unedited GluA2 mRNA, and although the unedited GluA2 accounted for no more than 30% of all GluA2 mRNA, these motor neurons underwent slow death (Hideyama and Kwak, 2011). Therefore, expression of unedited GluA2, even in a small proportion, is not favorable for the survival of motor neurons in mice and expression of ADAR2 sufficient to edit all the GluA2 mRNA rather than the expression level of ADAR2 per se is the critical factor for motor neuron survival. The critical role of GluA2 Q/R site-editing in neuronal death indicates that ALS motor neurons can survive, provided they express only edited GluA2, despite reduced ADAR2 activity. However, the expression level of ADAR2 likely decreases further with progression of the disease, and once the expression level of ADAR2 decreases below a threshold that is necessary to edit the Q/R site of all GluA2, motor neurons enter into a death cascade (see Fig. 5). This interpretation is consistent with the finding that the proportion of unedited GluA2 among all the GluA2 expressed in single neurons varied widely from 0% to 100% in a single ALS cases (Fig. 1C) (Kawahara et al., 2004a) and with the pathological finding that both healthy-appearing and shrunken motor neurons are observed in the ventral horn of the same ALS patients (Weller et al., 1997), as well. Therefore, it is likely that progressive downregulation of ADAR2 is closely relevant to the pathogenesis of ALS, in which the failure of A-to-I conversion at the GluA2 Q/R site is critical. We previously demonstrated that the threshold level of ADAR2 mRNA expression that enables editing of the Q/R sites of all GluA2 mRNA is approximately 20×10^{-3} relative to GluA2 mRNA in human brains (Kawahara et al., 2003a). We obtained consistent results in the present study; the expression level of ADAR2 mRNA in ALS^{edit} was well above this threshold

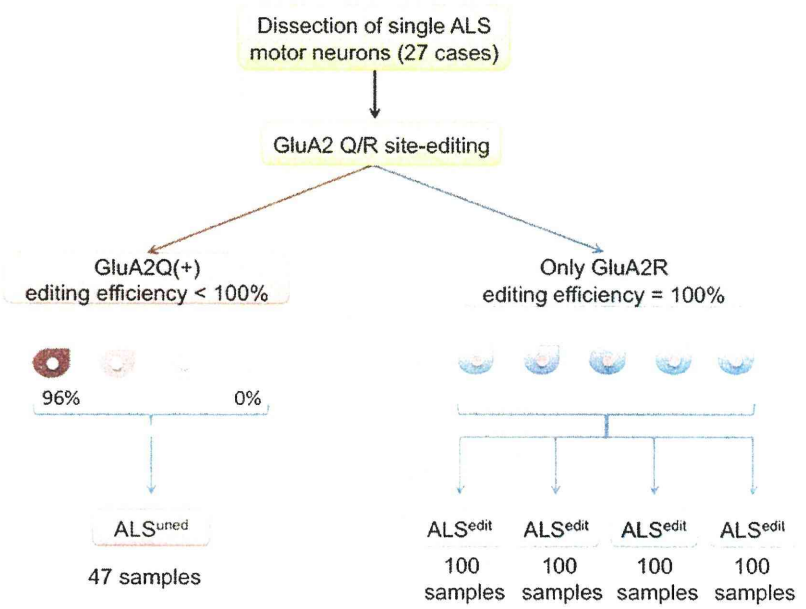

Fig. 3. Collection of ALS single motor neurons. We dissected single motor neurons from 27 sporadic ALS cases using a laser microdissector (see Table 1). After examining the efficiency of GluA2 Q/R site-editing in each lysate of a single motor neuron, we separately collected the remaining cDNA of the lysate that contained only Q/R site-edited GluA2 (ALS^{edit}) and lysate that contained unedited GluA2 mRNA (ALS^{uned}). Each ALS^{edit} contained cDNA from 100 motor neurons that expressed only Q/R site-edited GluA2 (n = 4), and one ALS^{uned} contained cDNA from 47 motor neurons that expressed unedited GluA2. ALS^{edit} and ALS^{uned} were used for analysis of the expression levels of ADAR1 mRNA and ADAR2 mRNA in ALS motor neurons shown in Figs. 2B and C.

($78.5\times10^{-3}\pm26.1\times10^{-3}$; range $60.0–117\times10^{-3}$), whereas the expression level in ALS^{uned} was far below this threshold (3.48×10^{-3}) (Figs. 2B and C).

In the present study, we showed that the expression level of ADAR2 mRNA is a factor regulating the ADAR2 activity in human spinal motor neurons, and that reduced expression level of ADAR2 transcripts was the cause of reduced ADAR2 activity in ALS motor neurons. We previously demonstrated that all the motor neurons express ADAR2 immunoreactivity in the spinal cord of normal human subjects, whereas approximately half of motor neurons lack ADAR2 immunoreactivity in patients with sporadic ALS (Aizawa et al., 2010). The present results provided us with knowledge that the lack of ADAR2 protein in ALS motor neurons resulted from reduced expression level of ADAR2 transcripts but not from accelerated degradation of ADAR2 protein, as shown in ischemic rat brain (Mahajan et al., 2011). Molecular mechanism regulating the level of ADAR2 mRNA expression and ADAR2 activity has been poorly elucidated. At least 48 different RNA variants are expressed in human brain, among which only three variants accounting for less than 10% of total amount of the transcripts encode active form of ADAR2 (Kawahara et al., 2005). Aside from the regulation by the expression level of ADAR2 mRNA, ADAR2 activity was positively regulated by the presence of inositol hexaphosphate in the catalytic domain (Macbeth et al., 2005) and negatively regulated by excessive expression of ADAR1 in glioma cells (Cenci et al., 2008) and cleavage of ADAR2 protein by Ca^{2+}-dependent protease (Mahajan et al., 2011).

Because ADAR2 is an RNA regulatory protein, the present findings support the emerging hypothesis that defects in RNA processing play a role in neurodegenerative diseases, including ALS (Lagier-Tourenne and Cleveland, 2009). For example, the mislocalization of TDP-43 and FUS/TLS has been reported in the motor neurons of ALS patients, including sporadic ALS. We previously found that ADAR2-deficient motor neurons exhibit TDP-43 pathology, whereas ADAR2-expressing motor neurons exhibit normal TDP-43 subcellular localization in sporadic ALS patients (Aizawa et al., 2010), indicating that there is a molecular link between these two RNA processing proteins. Whether TDP-43

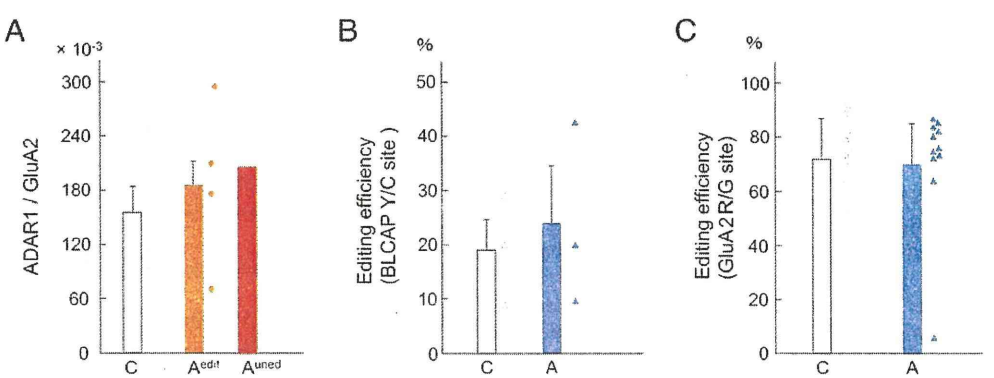

Fig. 4. Normal ADAR1 and ADAR3 in ALS motor neurons. (A) The expression levels of ADAR1 mRNA in ALS motor neurons, both ALS^{edit} (A^{edit}) and ALS^{uned} (A^{uned}) were in the same level as in control motor neurons (C). (B) Extents of RNA editing at the Y/C site of bladder cancer associated protein (BLCAP) mRNA in ALS AH did not differ from those in control AH. (C) There was no significant difference in editing efficiency at the R/G site of GluA2 mRNA in AH between ALS and control cases. Columns and bars represent mean ± SEM. Each triangle represents a value for the AH lysate, and each circle represents a value for the MN lysate from a single case.

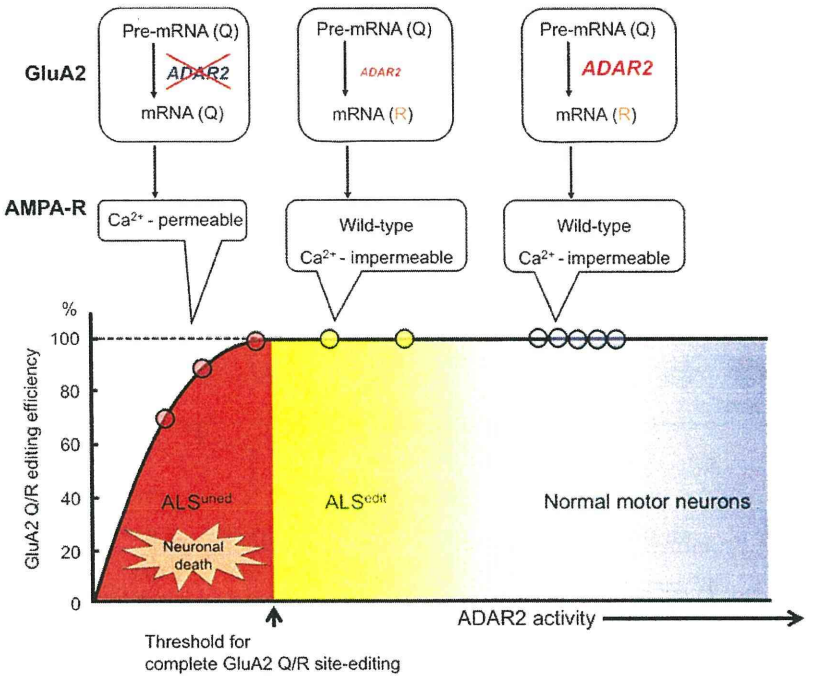

Fig. 5. Reduction of ADAR2 activity relative to expression of unedited GluA2 and death of motor neurons in sporadic ALS. ADAR2 activity was sufficiently high to edit the Q/R site of all the GluA2 mRNA expressed in the normal motor neurons (blue zone). In motor neurons of sporadic ALS, however, ADAR2 activity was lower than in normal motor neurons, even in those expressing only edited GluA2 mRNA (yellow zone). Motor neurons in which ADAR2 activity decreased below threshold (approximately 20×-10^{-3} relative to GluA2 mRNA) expressed Q/R site-unedited GluA2 and entered into the death cascade by expressing Ca^{2+}-permeable AMPA receptors containing GluA2 subunits unedited at the Q/R site (red zone).

pathology, including absence from the nucleus and mislocalization in the abnormal inclusion bodies, causes ADAR2 downregulation, or conversely ADAR2 downregulation causes TDP-43 pathology, remains to be elucidated. Recent microarray study demonstrated that ADAR2 mRNA was a target RNA of TDP-43 protein (Sephton et al., 2011) and ADAR2 gene expression was downregulated in the brain of TDP-43 knock-down animals (Polymenidou et al., 2011). Although these studies suggest that the reduction of ADAR2 expression resulted from the absence of TDP-43 in the nucleus of motor neurons with TDP-43 pathology, the quite modest extent of ADAR2 downregulation in the TDP-43 knock-down animal brain (Polymenidou et al., 2011) could not explain the loss of ADAR2-immunoreactivity in the motor neurons with TDP-43 pathology in patients with sporadic ALS (Aizawa et al., 2010). There remains a possibility that downregulation of ADAR2 causes TDP-43 pathology in ADAR2-lacking motor neurons. A close molecular link between ADAR2 downregulation and TDP-43 pathology in sporadic ALS is supported by the finding that neither inefficient GluA2 RNA editing nor mislocalization of TDP-43 occurs in SOD1 transgenic animals or SOD1-associated ALS patients (Kawahara et al., 2006; Mackenzie and Rademakers, 2007; Tan et al., 2007). These results suggest that death pathway involved in sporadic ALS including FTLD-MND is likely in common, while death pathway in SOD1-associated familial ALS may be one of other multiple different death pathways of motor neurons (Kwak and Weiss, 2006).

Because expression of ADAR2 was already reduced even in the motor neurons that express only edited GluA2 in ALS patients, downregulation of ADAR2 likely occurred before the onset of ALS symptoms and initiated the process of cell death when GluA2 RNA editing was incomplete. Therefore, investigation into the death cascade initiated by reduced ADAR2, including mislocalization of TDP-43, may provide insights into the pathogenesis of sporadic ALS. Unfortunately, little is known about the regulatory mechanism of ADAR2 expression in brains and spinal cords, and we do not know why ADAR2 is downregulated in ALS motor neurons. Because of the potentially critical role of ADAR2-mediated GluA2 RNA editing in sporadic ALS, elucidation of molecular mechanisms underlying ADAR2 downregulation is awaited. Demonstration of the disease-specific molecular abnormality that is involved in cell death provides a clue to the development of novel therapeutic strategies, and normalizing GluA2 Q/R site-editing in motor neurons is one potential method for treating sporadic ALS (Kwak et al., 2008).

Financial disclosures

The authors have no relevant financial disclosures.

Disclosure statement

The authors declare that there are no actual or potential conflicts of interest.

Acknowledgments

We thank Ms. K. Ito, Ms Y. Yamada, and Ms. T. Tanaka for technical assistance. This study was supported in part by Grants-in-Aid for Scientific Research from the Ministry of Health, Labor, and Welfare of Japan and from the Ministry of Education, Culture, Sports, Science, and Technology of Japan (SK), and Research Grants from Japan ALS Association and from The Nakabayashi Trust for ALS Research (TH). The authors declare that they have no competing interests.

Appendix A. Supplementary data

Supplementary data to this article can be found online at doi:10.1016/j.nbd.2011.12.033.

References

Aizawa, H., et al., 2010. TDP-43 pathology in sporadic ALS occurs in motor neurons lacking the RNA editing enzyme ADAR2. Acta Neuropathol. 120, 75–84.

Akbarian, S., et al., 1995. Editing for an AMPA receptor subunit RNA in prefrontal cortex and striatum in Alzheimer's disease, Huntington's disease and schizophrenia. Brain Res. 699, 297–304.
Brusa, R., et al., 1995. Early-onset epilepsy and postnatal lethality associated with an editing-deficient GluR-B allele in mice. Science 270, 1677–1680.
Burnashev, N., et al., 1992. Calcium-permeable AMPA-kainate receptors in fusiform cerebellar glial cells. Science 256, 1566–1570.
Cairns, N.J., et al., 2007. Neuropathologic diagnostic and nosologic criteria for frontotemporal lobar degeneration: consensus of the Consortium for Frontotemporal Lobar Degeneration. Acta Neuropathol. 114, 5–22.
Cenci, C., et al., 2008. Down-regulation of RNA editing in pediatric astrocytomas: ADAR2 editing activity inhibits cell migration and proliferation. J. Biol. Chem. 283, 7251–7260.
Chen, C.X., et al., 2000. A third member of the RNA-specific adenosine deaminase gene family, ADAR3, contains both single- and double-stranded RNA binding domains. RNA 6, 755–767.
Feldmeyer, D., et al., 1999. Neurological dysfunctions in mice expressing different levels of the Q/R site-unedited AMPAR subunit GluR-B. Nat. Neurosci. 2, 57–64.
Greger, I.H., et al., 2002. RNA editing at arg607 controls AMPA receptor exit from the endoplasmic reticulum. Neuron 34, 759–772.
Greger, I.H., et al., 2003. AMPA receptor tetramerization is mediated by Q/R editing. Neuron 40, 763–774.
Hideyama, T., Kwak, S., 2011. When does ALS start? ADAR2-GluA2 hypothesis for the etiology of sporadic ALS. Front. Mol. Neurosci. 33 Epub 2011 Nov 2..
Hideyama, T., et al., 2010. Induced loss of ADAR2 engenders slow death of motor neurons from Q/R site-unedited GluR2. J. Neurosci. 30, 11917–11925.
Higuchi, M., et al., 1993. RNA editing of AMPA receptor subunit GluR-B: a base-paired intron–exon structure determines position and efficiency. Cell 75, 1361–1370.
Higuchi, M., et al., 2000. Point mutation in an AMPA receptor gene rescues lethality in mice deficient in the RNA-editing enzyme ADAR2. Nature 406, 78–81.
Kawahara, Y., et al., 2003a. Low editing efficiency of GluR2 mRNA is associated with a low relative abundance of ADAR2 mRNA in white matter of normal human brain. Eur. J. Neurosci. 18, 23–33.
Kawahara, Y., et al., 2003b. Human spinal motoneurons express low relative abundance of GluR2 mRNA: an implication for excitotoxicity in ALS. J. Neurochem. 85, 680–689.
Kawahara, Y., et al., 2004a. Glutamate receptors: RNA editing and death of motor neurons. Nature 427, 801.
Kawahara, Y., et al., 2004b. Regulation of glutamate receptor RNA editing and ADAR mRNA expression in developing human normal and Down's syndrome brains. Dev Brain Res. 148, 151–155.
Kawahara, Y., et al., 2005. Novel splice variants of human ADAR2 mRNA: skipping of the exon encoding the dsRNA-binding domains, and multiple C-terminal splice sites. Gene 363, 193–201.
Kawahara, Y., et al., 2006. Underediting of GluR2 mRNA, a neuronal death inducing molecular change in sporadic ALS, does not occur in motor neurons in ALS1 or SBMA. Neurosci. Res. 54, 11–14.
Kwak, S., Kawahara, Y., 2005. Deficient RNA editing of GluR2 and neuronal death in amyotropic lateral sclerosis. J. Mol. Med. 83, 110–120.
Kwak, S., Weiss, J.H., 2006. Calcium-permeable AMPA channels in neurodegenerative disease and ischemia. Curr. Opin. Neurobiol. 16, 281–287.
Kwak, S., et al., 2008. Newly identified ADAR-mediated A-to-I editing positions as a tool for ALS research. RNA Biol. 5, 193–197.
Lagier-Tourenne, C., Cleveland, D.W., 2009. Rethinking ALS: the FUS about TDP-43. Cell 136, 1001–1004.
Levanon, E.Y., et al., 2005. Evolutionarily conserved human targets of adenosine to inosine RNA editing. Nucleic Acids Res. 33, 1162–1168.
Macbeth, M.R., et al., 2005. Inositol hexakisphosphate is bound in the ADAR2 core and required for RNA editing. Science 309, 1534–1539.
Mackenzie, I.R., Rademakers, R., 2007. The molecular genetics and neuropathology of frontotemporal lobar degeneration: recent developments. Neurogenetics 8, 237–248.
Mahajan, S.S., Ziff, E.B., 2007. Novel toxicity of the unedited GluR2 AMPA receptor subunit dependent on surface trafficking and increased Ca^{2+}-permeability. Mol. Cell. Neurosci. 35, 470–481.
Mahajan, S.S., et al., 2011. Exposure of neurons to excitotoxic levels of glutamate induces cleavage of the RNA editing enzyme, adenosine deaminase acting on RNA 2, and loss of GLUR2 editing. Neuroscience 189, 305–315.
Melcher, T., et al., 1996. A mammalian RNA editing enzyme. Nature 379, 460–464.
Nishimoto, Y., et al., 2008. Determination of editors at the novel A-to-I editing positions. Neurosci. Res. 61, 201–206.
Nutt, S., Kamboj, R., 1994. Differential RNA editing efficiency of AMPA receptor subunit GluR-2 in human brain. Neuroreport 5, 1679–1683.
Paschen, W., et al., 1994. RNA editing of the glutamate receptor subunits GluR2 and GluR6 in human brain tissue. J. Neurochem. 63, 1596–1602.
Polymenidou, M., et al., 2011. Long pre-mRNA depletion and RNA missplicing contribute to neuronal vulnerability from loss of TDP-43. Nat. Neurosci. 14, 459–468.
Riedmann, E.M., et al., 2008. Specificity of ADAR-mediated RNA editing in newly identified targets. RNA 14, 1110–1118.
Seeburg, P.H., 2002. A-to-I editing: new and old sites, functions and speculations. Neuron 35, 17–20.
Sephton, C.F., et al., 2011. Identification of neuronal RNA targets of TDP-43-containing ribonucleoprotein complexes. J. Biol. Chem. 286, 1204–1215.
Sommer, B., et al., 1991. RNA editing in brain controls a determinant of ion flow in glutamate-gated channels. Cell 67, 11–19.
Suzuki, T., et al., 2003. Recent advances in the study of AMPA receptors. Folia Pharmacol. Jpn. 122, 515–526.
Takuma, H., et al., 1999. Reduction of GluR2 RNA editing, a molecular change that increases calcium influx through AMPA receptors, selective in the spinal ventral gray of patients with amyotrophic lateral sclerosis. Ann. Neurol. 46, 806–815.
Tan, C.F., et al., 2007. TDP-43 immunoreactivity in neuronal inclusions in familial amyotrophic lateral sclerosis with or without SOD1 gene mutation. Acta Neuropathol (Berl). 113, 535–542.
Wang, Q., et al., 2004. Stress-induced apoptosis associated with null mutation of ADAR1 RNA editing deaminase gene. J. Biol. Chem. 279, 4952–4961.
Weller, R.O., et al., 1997. Diseases of muscle, In: Graham, D.I., Lantos, P.L. (Eds.), Greenfield's Neuropathology Vol 2, 6th. Arnold, pp. 489–581.
XuFeng, R., et al., 2009. ADAR1 is required for hematopoietic progenitor cell survival via RNA editing. Proc. Natl. Acad. Sci. U. S. A. 106, 17763–17768.

11

Objective Evaluation of the Severity of Parkinsonism Using Power-Law Temporal Auto-Correlation of Activity

Weidong Pan[1,3], Yoshiharu Yamamoto[2] and Shin Kwak[1]
[1]*Department of Neurology, Graduate School of Medicine, The University of Tokyo,*
[2]*Educational Physiology Laboratory, Graduate School of Education, The University of Tokyo,*
[3]*Department of Neurology, Shuguang Hospital Affiliated to Shanghai University of TCM,*
[1,2]*Japan,*
[3]*China*

1. Introduction

Parkinson disease (PD) is a neurodegenerative disorder not only with motor symptoms, including resting tremor, rigidity, bradykinesia and postural instability, but also with non-motor symptoms, including autonomic disturbance, sleep disturbance and depression. Due to the lack of objective biomarkers like the blood glucose level for diabetes mellitus, severity of parkinsonism has been evaluated by using the symptom-based Unified Parkinson Disease Rating Scale (UPDRS) (Martinez-Martin et al., 1994) that covers the various aspects of symptoms in patients with PD. Although the UPDRS is the standard method for the assessment of parkinsonism and the evaluation of drug effects, the scoring is not free from inter-rater variance or the fluctuation of the symptoms.

Wearable accelerometers enable long-term recording of patient's movement during activities of daily living, and hence might be a suitable device for quantitative assessment of the disease severity and progression. Alterations in locomotor-activity levels and disturbances in rest-activity rhythms have long been recognized as integral signs of major psychiatric and neurological disorders (Teicher, 1995; Witting et al., 1990). Improvement of ambulatory activity monitors (actigraph) has enabled precise calibration and storage of thousands of activity measurements acquired at predetermined times, hence enabled long-term recording of patient's movement during ordinary daily living (Katayama, 2001; Korte et al., 2004; Mormont et al., 2000; Okawa et al., 1995; Teicher, 1995; Tuisku et al., 2003; van Someren et al., 1996). It has been demonstrated that use of these devices is useful for the quantitative estimation of human behavior properties in normal subjects and patients with a variety of diseases, including depression, pain syndrome, and PD (Jean-Louis et al., 2000; Korszun et al., 2002; Nakamura et al., 2007; Ohashi et al., 2003; Pan et al., 2007; van Someren et al., 1993; 1998; 2006). However, because the pattern of daily activity greatly influences the recording with accelerometers, recorded activity levels may not adequately reflect the disease severity (Fig 1). Therefore, reliable analytical methods of the body acceleration signal free from the level of activity are required to describe the characteristics of body activity during daily living. Recently, fractal analysis was shown to be a robust tool to

disclose hidden auto-correlation patterns in biological data, such as heartbeat and limb movement (Ohashi et al., 2003; Pan et al., 2007; Peng et al., 1995; Sekine et al., 2004; Struzik et al., 2006). Power-law auto-correlation exponents for local maxima and minima of fluctuations of locomotor activity would be the most useful for our purpose, as they represent the level of persistency of movement patterns (Ohashi et al., 2003; Pan et al., 2007).

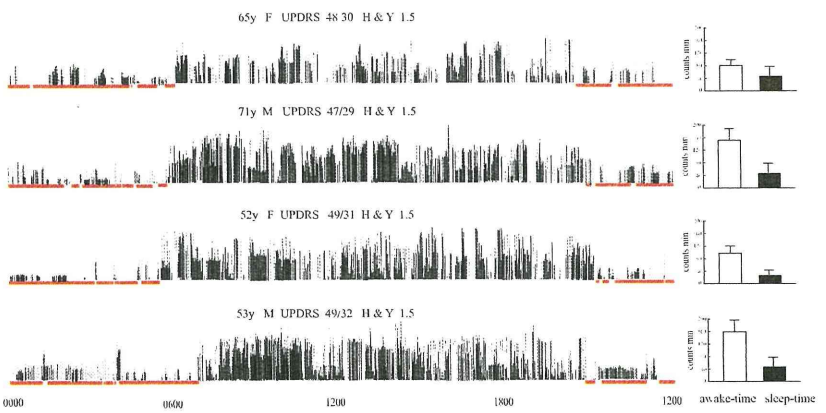

Fig. 1. Examples of 24 h actigraph recording. (left) Each vertical bar indicates activity counts per min. Sleep time is indicated in blue. Patients with approximately the same severity show different activity patterns and the activity counts (right: mean ± S.D.). UPDRS total/Part III.

In this review, we show how we can extract hidden autocorrelation patterns reflecting the severity of parkinsonism from the actigraph recording of patients' activity, and demonstrate that the analysis using power-law exponents is useful for the evaluation of effects of therapy on motor and non-motor symptoms of parkinsonism.

2. Analytical method of the motionlogger recordings for power-law auto-correlation exponents

We analyzed patients' physical activity records collected by an actigraph device using power-law exponents probing temporal auto-correlation of the activity counts. The power-law exponent for local maxima most sensitively and reliably reflects disability without being influenced by the presence of tremor or the patterns of daily living (Pan et al., 2007).

To examine temporal auto-correlation of the physical activity time series (i.e., *dynamic* aspects of physical activity), we used an extended, random-walk analysis, the detrended fluctuation analysis (DFA) (Peng et al., 1995), with a modification (Ohashi et al., 2003) for various "real-world" signals including activity time series. Briefly, a daytime physical activity time series was integrated, as in DFA, and wavelets with different time scales (S) were slid along the time series and correlated with the data to obtain the wavelet coefficients ($W(S)$) at each point. The third derivative of the Gaussian function was used as the so-called "mother wavelet":

$$\Psi(t) = t(3-t^2)e^{-0.5t^2}$$

where t is time. This is equivalent to using the Gaussian second derivative (so-called "Mexican hat") wavelet to examine the raw signals (Fig. 2), though the integration approach automatically removes the local mean and the local linear trend, as in DFA. By changing the scale of the wavelet, this "hat-shaped" template dilates or contracts in time, probing transient increases or decreases in activity records in different time scales. The transient increases (low-high-low activity patterns) yield local maxima of the wavelet coefficients at their time points, while the decreases (high-low-high activity patterns) yield local minima of the wavelet coefficients (see Fig. 2). Next, the squared wavelet coefficients at the local maxima or minima were averaged for all the available days. As the coefficient gives the magnitude of local fluctuations matching the shape of $\psi(t)$ with different time scales, the squared $W(S)$ was used, again as in DFA. Finally, the power-law exponent (α) was obtained separately for local maxima and minima as the slope of a straight line fit in the double-logarithmic plot of S vs. $W(S)^2$. This method yields the same α-values as does DFA (Ohashi et al., 2003), but separately for periods with higher and lower activity levels. The power-law (scaling) exponent, α, reflects the probability of a simultaneous increase or decrease in the variability at two distant points in time in the time series, applied to all distances up to *long-range* time scales, thereby probing the nature of "switching" patterns between high and low values in a statistical sense. Larger power-law exponents indicate positive temporal auto-correlation or *persistency* in the increase or decrease, and lower values correspond to negative auto-correlation or *anti-persistency* (Ohashi et al., 2003).

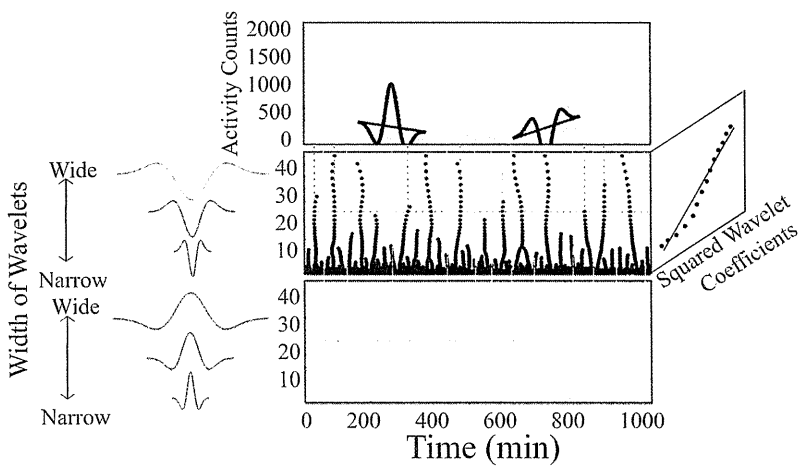

Fig. 2. Conceptual explanation of the method to obtain power-law exponents for local maxima and minima. (*top*) Various widths of hat-shaped wavelets are slid along the data to detect local minima (*middle*) and local maxima (*bottom*) of the wavelet coefficients. Note that the local minima and maxima appear at the transient decreases and increases of the activity, respectively. The power-law exponents are calculated from the slope of the log-log plot of squared wavelet coefficients vs. the scale for local minima and maxima. In the actual analysis, we used an integrated, rather than raw, time series and $\psi(t)$, i.e., the derivative of the "hat-shaped" wavelet. This yields the same power-law exponents as those obtained by the DFA method for the same local maxima and minima as obtained in this figure. Reprinted with permission from (Pan et al., 2007).

This method enables to evaluate relationships between time scales and magnitudes of fluctuation within each time scale, eliminating *non-stationarity* in the input data (i.e., changes in the baseline and trends within the data windows at different scales) that could affect calculation of the magnitudes of fluctuation. Therefore, this approach is suitable for the analysis of the long-term data collected in ambulatory settings (Pan et al., 2007).

3. Quantitative analysis of parkinsonism using power-law auto-correlation exponents

The data acquired during awake-time and sleep-time were separated with Action-W, Version 2 (Ambulatory Monitors Inc., Ardsley, NY) (Fig. 1) and the data during awake-time were used for analyses. Average wavelet coefficients for local maxima and minima of the severe and mild groups provided straight lines in the range of 8-35 min (Fig. 3A), indicative of very robust α-values. When the mean α-values for local maxima and minima were compared, they found a significantly lower α-value for local maxima in the mild group than in the severe group (Fig. 3B). All the patients (13 male and 9 female patients with Parkinson disease) in both the severe (Hoeh-Yahl score > 3.0; n=9)) and mild groups (H-Y score ≦ 3.0; n=10)) showed significantly lower α-values for local maxima on good-condition (GC) days than on bad-condition (BC) days that were classified according to diary scores, whereas there was no significant difference in the mean α-values for local minima (Fig. 3C).

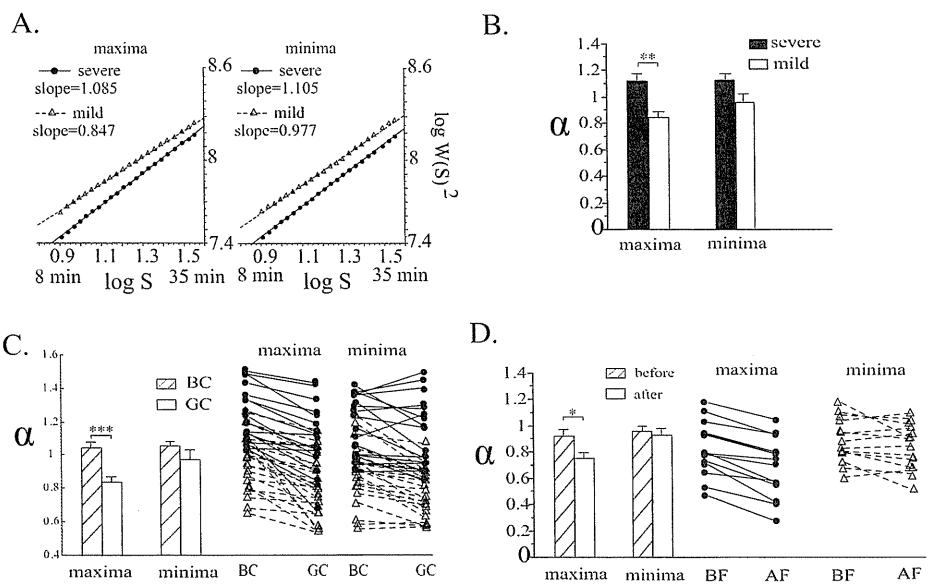

Fig. 3. Local maxima and minima of fluctuation of physical activity. (A) Average wavelet coefficients, as a function of the wavelet scale, for local maxima and minima. The slopes are power-law exponents, α. (B) Comparisons of the mean for the severe and the mild groups, (C) for BC and GC days and for individual patients, and (D) for days before and after antiparkinsonism medication and for each patient. *: $P < 0.05$, **: $P < 0.01$, and ***: $P < 0.001$. Reprinted with permission from (Pan et al., 2007).

When the effects of medication were examined, we found that all the patients who did not take any medication at the time of enrolement (n=6) showed lower α-values for local maxima on days more than three weeks after they received clinically effective anti-parkinsonism medication than on those before (Fig. 3D). Although presence of tremor significantly increased the activity counts in the arms with tremor as compared with those without tremor (Fig. 4A), power-law scaling of the records from arms with tremor showed a linear correlation between log S and log $W(S)^2$ in the range of 8 to 35 min (Fig. 4B) and α-values for local maxima were the same between the arms with tremor and those without tremor (Fig. 4B) with significantly higher α-values in patient arms than in control arms (Fig. 4C)

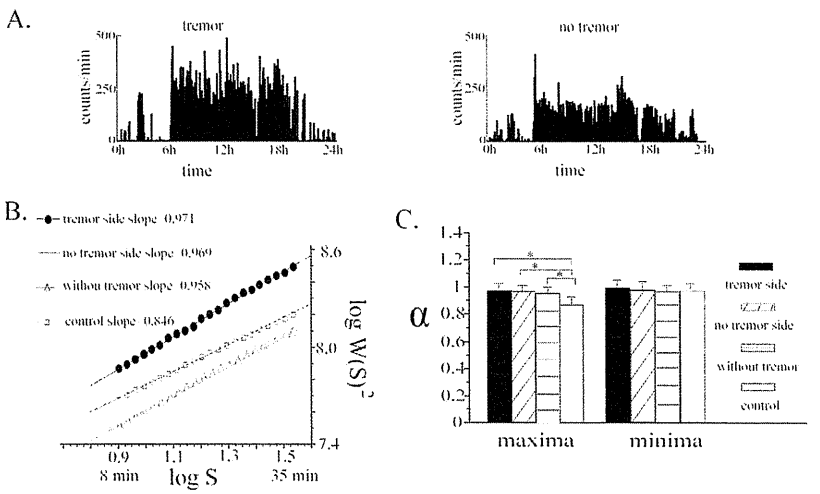

Fig. 4. Effects of tremor on actigraph counts and the power-law exponents. (A) Daily profiles of physical activity for the arm affected with tremor and that without tremor of a patient with unilaterally predominant parkinsonism with continuous tremor on one side. (B) Average wavelet coefficients for local maxima among arms with tremor (tremor) and without tremor (no tremor) of 6 patients with tremor, 26 arms of 13 patients without tremor (without tremor) and 20 arms of 10 control subjects (control). (C) The power-law exponents for local maxima and minima. *: $P < 0.05$. Reprinted with permission from (Pan et al., 2007).

Larger power-law exponents (α) indicate positive temporal auto-correlation, or *persistency*, in the increase or decrease in the variability of activity at two distant points in time in the time series, and lower values correspond to negative auto-correlation or *anti-persistency* (Ohashi et al., 2003). In other words, a lower α for local maxima or minima of activity records reflects more frequent switching behavior from low to high or high to low physical activity, respectively, and the switching behavior from lower to higher activity levels is considered to be related to akinesia in patients with parkinsonism. We found lower α-values for local maxima during GC days than during BC days, in the mild group than in the severe group, and before medication than after medication. Thus, these results demonstrate that the power-law analyses accurately describe the well known phenomenon that under these conditions patients switch their physical activity from lower to higher levels more easily, in